



A look into retinal organoids: methods, analytical techniques, and applications

Tess A. V. Afanasyeva¹ · Julio C. Corral-Serrano² · Alejandro Garanto^{3,4} · Ronald Roepman⁴ · Michael E. Cheetham² · Rob W. J. Collin¹

Received: 5 April 2021 / Revised: 14 July 2021 / Accepted: 9 August 2021 / Published online: 22 August 2021
© The Author(s) 2021

Abstract

Inherited retinal diseases (IRDs) cause progressive loss of light-sensitive photoreceptors in the eye and can lead to blindness. Gene-based therapies for IRDs have shown remarkable progress in the past decade, but the vast majority of forms remain untreatable. In the era of personalised medicine, induced pluripotent stem cells (iPSCs) emerge as a valuable system for cell replacement and to model IRD because they retain the specific patient genome and can differentiate into any adult cell type. Three-dimensional (3D) iPSCs-derived retina-like tissue called retinal organoid contains all major retina-specific cell types: amacrine, bipolar, horizontal, retinal ganglion cells, Müller glia, as well as rod and cone photoreceptors. Here, we describe the main applications of retinal organoids and provide a comprehensive overview of the state-of-art analysis methods that apply to this model system. Finally, we will discuss the outlook for improvements that would bring the cellular model a step closer to become an established system in research and treatment development of IRDs.

Keywords Retina · Organoid · Inherited · Omics · Degeneration · Therapy

Introduction

Inherited retinal diseases (IRDs) comprise a genetically and clinically heterogeneous subgroup of vision disorders with over 270 different causative genes identified so far [1]. Many IRDs are characterised by progressive loss of photoreceptors

or the underlying retinal pigment epithelium (RPE) that can lead to severe visual impairment. While significant progress has been made to date, the majority of these blinding diseases remains untreatable.

With the notable example of the FDA approval of a gene augmentation therapy for *RPE65*-associated IRD, recent success in the field of gene augmentation therapies is largely driven by preclinical studies performed in animal models [2–4]. Despite their advantages, such as low cost and ease of genetic manipulation, each animal model also has disadvantages; for example, differences in retinal anatomy, photoreceptor types, or genomic conservation compared to a human, alongside ethical restrictions [5].

In vitro models are becoming an increasingly popular addition to animal models [6]. For example, induced pluripotent stem cells (iPSC) derived from somatic cells of an individual can be genetically reprogrammed to become pluripotent, meaning that they can differentiate into any other adult cell type [7]. Differentiated cells that are generated from these iPSCs contain the unique genome of the individual and, therefore, have the exact genetic and cellular context to study disease mechanisms of hereditary disorders. In the case of photoreceptor-based IRDs, photoreceptors in iPSC-derived retinal organoids will recapitulate many of

Michael E. Cheetham and Rob W. J. Collin shared last authors.

✉ Michael E. Cheetham
michael.cheetham@ucl.ac.uk

✉ Rob W. J. Collin
rob.collin@radboudumc.nl

- ¹ Department of Human Genetics and Donders Institute for Brain, Cognition and Behaviour, Radboud University Medical Center, Geert Grooteplein 10, 6525 GA Nijmegen, The Netherlands
- ² UCL Institute of Ophthalmology, 11-43 Bath Street, London EC1V 9EL, UK
- ³ Department of Pediatrics, Amalia Children's Hospital and Radboud Institute for Molecular Life Sciences, Radboud University Medical Center, Nijmegen, The Netherlands
- ⁴ Department of Human Genetics and Radboud Institute for Molecular Life Sciences, Radboud University Medical Center, Nijmegen, The Netherlands

the pathophysiological processes, both at the cellular and molecular levels that underlie the disease in the respective IRD patients.

The retina is a light-sensitive neural tissue situated at the back of the eye that displays a laminated appearance upon transverse sectioning and light microscopy. At the most posterior part resides the layer of RPE. The basal surfaces of the RPE cells face the choroidal blood vessels, whereas their apical processes interdigitate with photoreceptors. The specialised light-sensing photoreceptor outer segments (OS) form the next layer and are connected to their adjacent biosynthetic inner segments by the connecting cilium. The outer limiting membrane (OLM), a barrier to movement in the extracellular space formed by the photoreceptor and Müller cell end-feet, separates the inner segments from a layer containing the nuclei of rod and cone photoreceptors, called the outer nuclear layer (ONL), whereas photoreceptor axons and processes meet with horizontal and bipolar cells in the outer plexiform layer (OPL). More anterior, the inner nuclear layer (INL) harbours nuclei of the bipolar, amacrine, horizontal, and Müller cells, while the inner

plexiform layer (IPL) contains the processes and synapses of bipolar and amacrine with retinal ganglion cells (RGC). The nuclei of RGCs form the RGC layer while their axons form the optic nerve fibre layer. The most anterior layer is populated by astrocytes that form an inner limiting membrane (ILM), separating the retina from the vitreous [8]. During the early embryonic development of the foetal eye, the retina is formed from neuro-ectoderm, the outermost embryonic germ layer. The ectoderm forms two optic vesicles, the distal portion of which folds inward to form the optic cups. The outer and inner walls of an optic cup generate RPE and retina, respectively [9].

Retinal organoid differentiation resembles the formation of the optic vesicle. After a prolonged culture using state-of-the-art protocols, retinal organoids can contain most of the retinal neuronal cell types such as rods and cones, ganglion, bipolar, horizontal, amacrine, and Müller cells, as well as, mimicking the lamination of the retina with most of the photoreceptor nuclei placed in the ONL, with infrequent misplaced cones appearing in the INL (Fig. 1) [10–17].

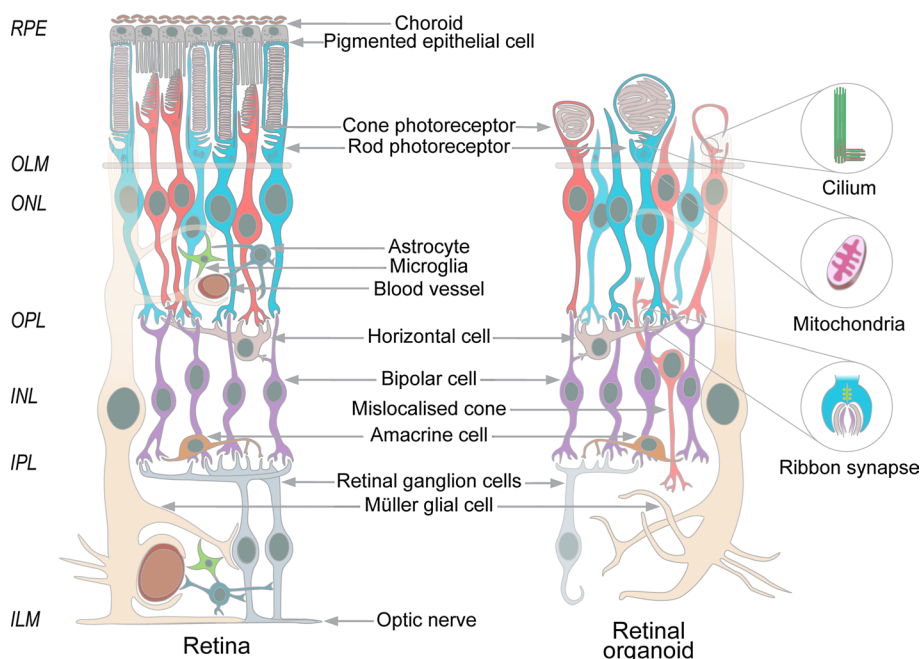
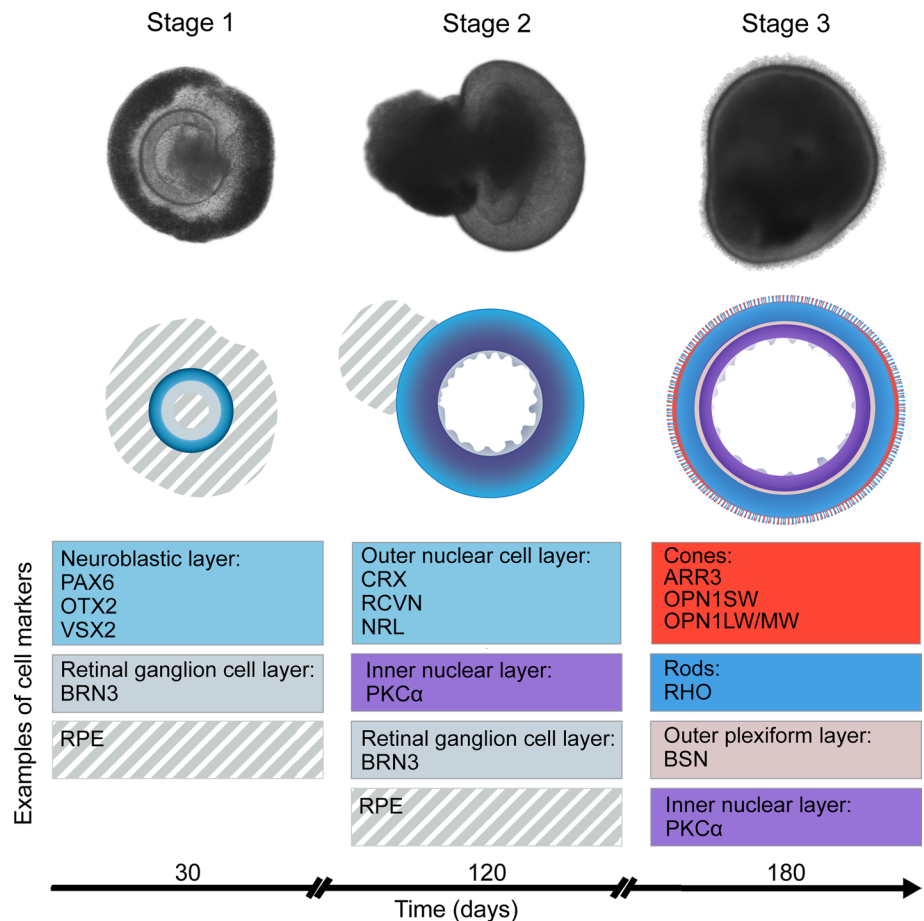


Fig. 1 The cellular organization of the retinal organoids mimics the organization of the retina and contains most of the retinal neuronal cell types, such as most posterior RPE (grey), which faces choroidal blood vessels (brown) at the basal and cones (red) and rods (blue) at the apical sides. The outer limiting membrane (OLM) (tan) is formed by the Müller cell end-feet (cream) and photoreceptors. The photoreceptor nuclei constitute a layer called the outer nuclear layer (ONL), whereas their axons and processes meet with horizontal (pink) and bipolar cells (purple) in the outer plexiform layer (OPL). More anterior, the inner nuclear layer (INL) harbours nuclei of the bipolar (purple), amacrine (orange), horizontal cells (pink), and Müller glia

(cream), while the inner plexiform layer contains the processes and synapses of bipolar cells (purple), amacrine cells (orange), and RGC that are reduced in number by the stage of photoreceptor maturation (grey). In retinal organoids, subcellular structures specific to the retina were observed such as outer segments (OS), inner segments (IS), and connecting cilia with basal bodies, mitochondria, and ribbon synapses (right panels). In contrast to the retina, the retinal organoids can contain cone photoreceptors in the INL and do not contain choroid, blood vessels, astrocytes (dark blue), microglia (green), and the defined RPE layer

Fig. 2 At different maturation stages the retinal organoid contains a progressively complex population of cells. Upper row shows bright field microscopy of retinal organoids at different stages of development. Middle row schematics showing the cellular composition. Lower row shows commonly used markers to identify the different cell types. Colour coding, neuroblastic (pale blue), RGC (grey), inner nuclear layer (bipolar cells, purple), cones (red), rods (blue)



Three differentiation stages of a retinal organoid can be described (Fig. 2). At stage 1, around differentiation day (D) 30 to 50, organoids develop a clear phase-bright outer neuroepithelial rim that contains neural retina progenitors and the inner part of the organoid harbours RGCs. RGCs are the first retinal cells to differentiate at around D50, but their numbers decrease from D90 onwards, seemingly due to the lack of connection to brain targets [11, 17]. A recent paper showed that in assembloid culture, where retinal and brain organoids were fused at D50, RGCs exhibited axonal outgrowth and pathfinding into the cortical neurons of brain organoids, alongside increased proliferation and decreased cell death at D150 [18]. At stage 2, around D80-D120, organoids develop a phase-dark core with a reduced bright rim and early progenitors of cones and rods begin to appear. At stage 3, around D120-180, the outer rim is more visible with hair-like, or brush-border-like structures that correspond to the photoreceptor inner and outer segments [10]. The differentiating retinal organoid expresses a specific set of biomarkers at each maturation stage; for example, photoreceptors express field transcription factor PAX6, and retinal progenitor cell factor VSX2 early in differentiation, followed by a photoreceptor precursor-specific transcription factor CRX, early rod-specific marker NRL, and the mature

cone and rod markers recoverin, and L/M/S-opsins and rhodopsin, respectively. Photoreceptor cilium and OS formation during retinal development can be tracked by staining of the PCARE protein from D120-180 [19]. A dark patch of RPE cells is frequently observed as part of the developing neural-retinal vesicle, but not as a monolayer overlying the neural retina. The retinal organoid cell populations are considered to be fully developed between D210 and D260, and decrease in complexity from there on [10, 11].

Methods of retinal organoid differentiation

Important advances have been made in the development of protocols that are used to differentiate stem cells into retinal cells, improving the formation of well-defined retinal cell types and structures, as well as the efficiency and reproducibility (Table 1).

One of the earliest successful differentiation methods used adherent (2D) cultures to direct embryonic stem cells into an anterior neural fate. Adding Wnt/BMP signalling inhibitors alongside IGF-1 to the media, induced the formation of photoreceptor-marker positive cells, but these were not the main cell types in the adherent culture [20]. Inhibition of Notch signalling with DAPT treatment significantly

Table 1 Breakthrough methods for differentiation of germline stem cells into retinal organoids

Initial cell type	NRV's formation method	Neural induction media	Retinal differentiation media	Photoreceptor markers	Outer segments	Comment	References
hESCs	EB formation and transferred to adherent culture	D1–D3: DMEM:F12, 10% KSR, B27, 1 ng/mL noggin, 1 ng/mL Dkk1, 5 ng/mL IGF-1	D4–D91: DMEM:F12, B27, N2, 1 ng/mL noggin, 1 ng/mL Dkk1, 5 ng/mL bFGF	RHO, OPN1SW, NRL	Not present	First 2D method to derive retinal cells from embryonic stem cells	[20]
mESCs, mkESCs, *hESCs	EB formation and transferred to adherent culture	D1–D2: DMEM/F12 0.1 mM NEAA, 0.1 mM β -met, 20% KSR, 2 mM L-glutamine D3–D6: G-MEM, 0.1 mM NEAA, 0.1 mM β -met, 20% KSR, 1 mM pyruvate KSR, 1 mM pyruvate D7–D14: 15% KSR D0–D20: Dkk-1 (100 ng/ml), Lefty-A (500 ng/ml)	D14–D90/D120: GMEM, NEAA, 0.1 mM β -met, 10% KSR, 1 mM pyruvate D90/D120–D200: GMEM, 5% KSR, NEAA, 1 mM pyruvate, 0.1 mM β -met, 1 μ M RA, 100 μ M taurine, N2	RHO, RCVRN, OPN1LW, OPN1MW, OPN1SW	Not characterised	Inhibition of Notch with DAPT, addition of RA and taurine to increase photoreceptor production	[21]
mESCs	EB formation	D0–D7: GMEM + 1.5% KSR, NEAA, 1 mM pyruvate, 1 mM β -met	D7–D10: DMEM/F12 + N2 D10–D35: DMEM F12 + N2 + 10% FBS + 0.5 μ M RA + 1 mM taurine D16: + DAPT	RCVRN, RHO	Not characterised	First 3D method using mouse cells	[23]
hESCs	EB formation	D0–D12: GMEM, 20 μ M Y-27632 20% KSR, NEAA, 1 mM pyruvate, 0.1 mM β -met, 3 μ M IWR1e D12–D18: + 10% FBS D15–D18: + 3 μ M CHIR99021, 100 nM SAG	D18–D121: DMEM/F12-glutamax (3:1), N2, 10% FBS, 0.5 μ M RA D121–126: w/o RA	NRL, RCVRN, RHO, OPN1SW	Apical protrusions of mono-ciliated, rich cell bodies, reminiscent of inner segments (ellipsoids), which carry connecting cilia OS formation	Improvement of the 3D method using human cells	[24]
hiPSCs	EB formation	D1: mTesR/NIM (DMEM/F12 1:1, N2, NEAA, 2 μ g/mL heparin) 3:1 D2: mTesR1/NIM 1:1 D3–D15: 100% NIM	D16–D41: DMEM/F12 3:1, B27, NEAA D42–D63: DMEM/F12 3:1, B27, NEAA, 10% FBS, glutamax, 100 μ M taurine D63–D91: + 1 μ M RA D92–end: + 0.5 μ M RA	RHO, OPN1LW, OPN1MW, OPN1SW	Present with connecting cilia and basal bodies. Occasionally showing light response in vitro	First 3D/2D method to describe mature and light-responder photoreceptor cells	[17]

Table 1 (continued)

Initial cell type	NRV's formation method	Neural induction media	Retinal differentiation media	Photoreceptor markers	Outer segments	Comment	References
hiPSCs	Adherent culture, NRV excision and grown in suspension	D2–D14: DMEM/F12 1:1, NEAA, N2 D14–D21: +10 ng/mL FGF2 D21: w/o FGF2 D21–D28/D28–D35: +10 μ M DAPT	D14–D112: DMEM/F12 1:1, NEAA, N2	Photoreceptor positive markers in inter-nal rosettes of the organoids: recoverin, OPN1LW, OPN1MW	Positive for the ciliary marker acetylated tubulin. No OS visible	First 2D/3D method including NRV excision	[25]
hESCs	EB formation	D0–D18: 45% IMDM, 45% F12-Ham, glutamax, 10% KSR, 10 μ M 1-thioglycerol, 1% chemically defined lipid concentrate D0–D6: +20 μ M Y27632 D6–D16: +1.5 nM BMP4	D18–D150: DMEM-F12-glutamax, 1% N2, 10% FBS, 0.5 μ M RA, 0.1 mM taurine D18–D24: +3 μ M CHIR99021, 5 μ M SU5402 (for RPE induction)	NRL, RCVRN positive photoreceptors	Not characterised	Addition of BMP4 increases the formation of neuroretinal epithelium	[30]
hESCs	EB formation	D0–D13/D17: DMEM/F12 + glutamax: neurobasal medium 1:1, 0.5X B27, 0.5 XN2, 0.1 mM β -met, 2 mM glutamax	D13/D17–D27/31: DMEM/F12 (3:1), B27 (w/o vit A), NEAA D27/D31–D187: DMEM/F12 (3:1), B27, NEAA, 10% FBS, 100 μ M taurine, 2 mM glutamax	RHO, OPN1LW, OPN1MW, OPN1SW	Present with connecting cilia, basal bodies and membrane disks	Spontaneous formation of neuroretinas	[27]
hESCs	Adherent culture, NRV excision and grown in suspension	D3–D28/D49: DMEM/F12 1:1, N2, NEAA, glutamax	D28/D49–D63: DMEM/F12 3:1, B27, 10% FBS, 100 μ M taurine, glutamax D63–D84: +1 μ M RA D84–end: +0.5 μ M RA, +N2	RHO, OPN1LW, OPN1MW, ARR3, PRPH2, RIBEYE, SYNTAXIN3	Present with disorganised disk membranes, connecting cilia and basal bodies	Improvement of the 2D/3D combination model	[26]
hESCs, hiPSCs	EB formation	D1–D6: DMEM/F12 (1:1), N2, NEAA, glutamax, 2 μ g/mL heparin D6: +1.5 nM BMP4	D16–D25/D30: DMEM/F12 3:1, B27, NEAA, glutamax D25/D30–D100: +5% FBS, 100 uM taurine, 1 μ M RA, 1:1000 lipid supplement D100: w/o RA	RHO, RCVRN, OPN1LW, OPN1MW, OPN1SW, NR2E3, NRL, ARL13B, ARR3	Present with partially stacked disks, connecting cilia, basal bodies	Development of a practical staging system of the retinal organoids. Demonstration that BMP4 increases NRV formation. Adaptation from [17] and [30]	[10]

Table 1 (continued)

Initial cell type	NRV's formation method	Neural induction media	Retinal differentiation media	Photoreceptor markers	Outer segments	Comment	References
hESCs, hiPSCs	EB formation	D1: E8/NIM 3:1, N2, 2 µg/mL heparin, NEAA D2: E8/NIM 1:1, N2, 2 µg/mL heparin, NEAA D3–D16: 100% NIM	D16–D42: DMEM/F12 3:1, B27, NEAA D42–D63: + 10% FBS, 100 mM taurine, glutamax D63–D92: + 1 µM 9-cis retinal D92–end: + 0.5 µM 9-cis retinal, N2	RHO, OPN1LW, OPN1MW, OPN1SW	Present with connecting cilia and basal bodies	Accelerated photoreceptor differentiation by 9-cis retinal. Adaptation from [17]	[34]
hiPSCs	EB formation	D1–D16: DMEM/F12 (1:1), glutamax, 24 nM sodium selenite, 16 nM progesterone, 80 µg/ml human holotransferrin, 20 µg/ml human recombinant insulin, 88 µM putrescin, NEAA	D16–D40: DMEM/F12 (3:1), B27, NEAA D24: 10 µM Y-27632 D40–D70: + 10% FBS, 100 µM taurine D70–D100: + 1 µM RA D100–D190: + 0.5 µM RA D190–End: w/o RA	RHO, PNA lectin, ROM1	Present with connecting cilia and basal bodies	Generation of retina-on-chip model. Adaptation from [17]	[172]
hESCs	EB formed and maintained in suspension	D1–D18: VNIM (DMEM/F12, 20% KOSR, L-Glutamine, NEAA, B27, IGF-1 (5 ng/mL)) D18–D37: + 0.5 uM RA, IGF-1 (5 ng/mL), T3 (40 ng/mL), Taurine (0.1 mM) D1–D2: + 10 µM Y27632	D37–D120: DMEM/F12, L-Glutamine, NEAA, B27, N2, IGF-1 (10 ng/mL)	RCVRN, RIBEYE, RHO, OPN1LW, OPN1MW	Not characterised	Demonstration that IGF-1 increases the formation of laminated NRVs. Adaptation from [185] following [31]	[32]

The table includes details of the culturing media and reagents used in each protocol for better comparison. Briefly, the majority of protocols use DMEM/F12 as medium base, commonly using the differentiating factors serum, RA, taurine, B27 and/or N2. Non-essential amino acids (NEAA) and glutamax supplements are often included. Small molecules such as IGF1, BMP4, heparin, CHIR99021 or DAPT, may be added at specific time points to regulate differentiation signalling pathways. RA retinoic acid, β -mercaptoethanol, NIM neural induction medium. *Differentiation protocol described for this initial cell type

increased the proportion of photoreceptor and RPE cells, and the addition of the rod-genesis factors retinoic acid (RA) and taurine boosted the number of photoreceptor-marker positive cells [21]. Neural induction media with heparin and chemically defined N2 supplement nudged iPSC to aggregate into embryoid bodies, which then adhered to the surface of the coated culture dish and differentiated towards neural retina [22]. However, the number of photoreceptors obtained under these conditions was low, these photoreceptors were mainly precursor cells, and were distributed in a monolayer of mixed cultures.

A key step to obtain stratified neural retinas was the transition to non-adherent (3D) protocols. Mouse embryonic stem cell (ESC) aggregates cultured in suspension under low-growth factor conditions together with Matrigel matrix improved the formation of optic cups mimicking the embryonic optic cup with apical-basal polarities [23]. The addition of foetal bovine serum (FBS) and the hedgehog agonist SAG augmented retinal differentiation for human stem cells with laminated retinas, expressing markers of all retinal cell types: ganglion, amacrine, bipolar, horizontal, Müller, and photoreceptor cells. In human ESC-derived retinal organoids, electron microscopy (EM) analysis of the photoreceptor cell layer showed mitochondria and rudimentary connecting cilia with basal bodies, only lacking obvious OS [24].

A combination of 3D and 2D protocols that did not require the addition of small molecules differentiated iPSCs to mature and light-responsive photoreceptor cells with rudimentary OS. This was achieved by reducing the RA concentration between D50 and D70, and prolonging the culturing times [17]. Alternatively, a 2D to 3D approach enabled the bypass of embryoid body formation, generating neuroretinal structures in the adherent culture that were excised and further cultured in suspension [25]. These floating neuroretinas formed neural rosettes containing photoreceptors, but without the characteristic lamination of other 3D cultures. Incorporation of the differentiating retinal factors—serum, RA, taurine, and the supplements N2 and B27—permitted generation of photoreceptors with rudimentary OS visible at the edges of the retinal organoid [26]. Interestingly, a different procedure to the 2D and 3D models generated neuroretinas with mature photoreceptors following spontaneous attachment and spreading of epithelial structures, called cysts [27].

Most of these protocols share common media components, but a switch in the timing and addition of certain molecules helped to improve the yield of neuroretinal vesicles obtained. Bone morphogenetic proteins play a role in establishing dorsal/ventral patterning of the retina [28], and specifically, BMP4 is needed for retina specification in mice [29]. The addition of timed BMP4 treatment was shown to increase the self-formation of neuroretinal epithelia [10, 30]. The factor IGF-1 also facilitated the formation

of 3D-laminated retinal organoids when added to the media during the first 3 months of differentiation [31, 32]. Nevertheless, this response to BMP4 and IGF-1 activation is iPSC line- and differentiation method-dependent [33]. Addition of 9-cis retinal, instead of the widely used all-trans RA, accelerated rod photoreceptor differentiation in organoid cultures, with higher rhodopsin expression and more mature mitochondrial morphology evident by D120 [34]. For cone specification, thyroid hormone signalling regulation helped to control the fate of cone subtypes in retinal organoids [12]. RGCs usually appear at D40 to D50 after the start of differentiation. Accelerated ganglion cell development within D28 of differentiation was achieved by encapsulating EBs in a 3D Matrigel drop instead of growing in suspension [35].

Current applications for retinal organoids

Retinal organoid technology offers the possibility to obtain retinal tissue for a wide range of applications and research questions. To illustrate, here we highlight the potential of retinal organoids for therapeutic transplantation and as a model to assess therapeutic strategies.

Retinal organoids as a source for transplantation

Photoreceptors are often the first cell type lost in many retinal diseases. When that occurs and the adjacent retinal layers remain intact, transplantation of healthy photoreceptors could be a potential treatment option. Photoreceptors derived from human stem cells are an exceptional and unlimited source of human cells for transplantation. Transplanted photoreceptors were first thought to integrate into the ONL of degenerating retina and improve vision in mouse models [36, 37]. However, recent studies have demonstrated that transplanted photoreceptors do not integrate; instead, they remain in the subretinal space and exchange cytoplasmic material with the host cells [38–41]. In light of this discovery, earlier publications should be interpreted with caution and new carefully designed studies are required to clarify if integration or material transfer are mediating the observed effects.

Transplanted embryonic stem cell-derived photoreceptors from 2D cultures into adult *Crx*^{-/-} mice retinas were able to produce ERG responses [42]; however, the photoreceptors used in this study did not mature to form OS. The advent of 3D protocols to generate retinal organoids [17, 23, 24] offered the opportunity to obtain a better yield and reproducibility of photoreceptors. For example, transplantation of mouse ESCs-derived photoreceptors by subretinal injection into *Gnat*^{-/-} mice displayed features of mature photoreceptors, such as inner and outer segments. When transplanted to *Rho*^{-/-} and *Prph2*^{-/-} mutants, the donor cells showed rhodopsin and PRPH2 positivity that were lacking in the

endogenous retinas, although they did not contain OS [43]. Transplantation of cones purified from retinal organoids into adult *Nrl*^{-/-} mice, a model where rod cells take a different fate and become S-cones [44] was reported to be successful [26]. Donor L/M cones were well oriented in the ONL and expressed markers of the mature cell type. In adult an LCA4 model, *Aipl1*^{-/-} mice that lack photoreceptors transplanted L/M cones expressed the presynaptic protein ribeye and photopigments. However, the functionality of these cells was not assessed [45].

The source and developmental stage of transplanted cells, as well as their enrichment and delivery methods, are key to successful transplantation. The body of photoreceptor precursor cell isolation and transplantation work suggests that fully mature photoreceptors may be more fragile and unfit for transplantation than retinal progenitor cells. Fluorescence-activated cell sorting (FACS) of the progenitor cell marker C-kit, a type III receptor tyrosine kinase, and the pluripotency marker SSEA4, can be used to isolate retinal progenitor cells without tumorigenic components [46, 47]. C-Kit⁺/SSEA4⁻ cells possess the characteristics of retinal progenitors and in *rd1* mice, organoid-derived C-kit⁺/SSEA4⁻-transplanted cells protected the ONL and improved visual function. The photoreceptor-specific cell surface markers CD24 and CD73 can also be used to isolate photoreceptors [48, 49]. Label-free techniques of photoreceptor selection that comply with current good manufacturing practices (cGMP) are preferred for clinical translation. Magnetic activated cell sorting (MACS) based on CD73 expression allows for enrichment of rod photoreceptor precursors [50]. Photoreceptors from retinal organoids can also be isolated using a panel of biomarkers [51]. Microfluidic enrichment of photoreceptor precursor cells is a more recent approach that allows to separate RPE cells from the rest of retinal cells based on their mechanical and physical properties. The device was also able to separate some rods from cones, although further improvements will be needed to filter bipolar and ganglion cells [52]. Depending on the disease, the stage of the disease, and the cell type to be transplanted, different delivery methods need to be considered. Trans-scleral and transvitreal injection are effective methods to deliver retinal cells into the eye, with the transvitreal approaches preferred in the clinic [53]. Integration and survival of photoreceptor cells in suspension is limited compared to the more successful transplant of RPE cells [41, 54, 55].

Transplantation of retinal sheets is an alternative to single-cell suspension transplants. Transplanted mouse iPSCs-derived retinal sheets can survive in the subretinal space of *rd1* mice and form synaptic connections with the host retina [56]. The hESC-derived retina can mature and form an ONL with photoreceptor inner and outer segments after transplantation in monkeys and nude rats [57]. The same group demonstrated that the transplanted cells were able

to respond to light [58]. Transplanted sheets formed neural rosettes and improved visual function in the host retina of immunodeficient Rho^{S334ter-3} rats, a model of severe retinal degeneration [59]. hESC-derived D60-D70 full retinal organoids implanted into the subretinal space of immunosuppressed wild-type cats integrated and formed cytoplasmic and synaptic interactions with the host tissue [60]. Transplantation of iPSCs-derived retinas formed rosettes bearing photoreceptors with OS, bipolar, and amacrine cells, but no RGCs. Grafted cells formed synapses with the host bipolar cells and generated light-responses. These cells survived after 5 months in rats, and over 2 years in monkeys, demonstrating the long-term potential of this therapeutic approach [61].

Other physical factors may play an important role in transplantation. The OLM is made of cadherin–catenin complexes that mediate cell–cell adhesion and serves as a barrier for the integration of transplanted photoreceptor precursor cells [62]. Disruption of OLM proteins enhanced integration of transplanted photoreceptors [63]. Gliosis caused by reactive Müller cells might be considered as well in the context of transplantation and OLM as a barrier [64].

Despite these advances and the availability of well-characterised GMP-compliant retinal cells via stem cell differentiation, there are still many challenges to be overcome to achieve the level of successful transplantation that is needed to restore high acuity vision.

Retinal organoids to assess therapeutic strategies

Therapies based on adeno-associated virus (AAV) vectors are gaining momentum as a potential treatment for retinal diseases. One major reason is the accessibility of the eye, which makes it suitable for intravitreal or subretinal injection surgery. AAVs can infect human cells, allowing long-term expression of the transgene after a single dose.

There are several known AAV serotypes [65], with different tropisms for the tissue they can infect. AAV serotype 2 has been widely used in the eye [66]. Human retinal organoids offer an opportunity to investigate viral tropism and transduction in tissue that resembles the human retina. The first evaluation of different AAV serotypes in retinal organoids showed that AAV2/8 and ShH10 (an AAV6 variant) [67] were the most robust to transduce photoreceptors in this system, with higher efficiency of the latter [68]. The promoter rhodopsin kinase was able to drive expression in both rod and cone photoreceptors, while the opsin 2.1 promoter was active in L/M-cones and some S-cones [68]. The AAV serotype AAV2-7m8 in combination with opsin 1.7 promoter was effective in the transduction of L/M-cones [69]. Compared to AAV2, AAV9, and AAV8, AAV2-7m8 demonstrated higher tropism for photoreceptor precursor cells at D44 of differentiation and remained stable for at

least 4 weeks [70]. AAV2/5 under the CAG promoter transduced photoreceptors with high efficiency (~90%) and was used to rescue RP2 expression in RP2-KO retinal organoids, improving photoreceptor survival [71]. On the retina-on-chip model, the AAV2-7m8 variant was also more efficient at transducing mature photoreceptors, Müller, and ganglion cells, compared to first-generation AAV variants [72]. The newly generated recombinant AAV vectors AAV2.NN and AAV2.GL outperform AAV2 and AAV2-7m8 in mice and are able to effectively transduce human retinal explants [73]. In organoids, the variant AAV2.GL had a comparable transduction efficiency to AAV2-7m8, while AAV2.NN had higher fluorescence levels than all other AAV variants tested [72]. The NN peptide-insert also showed high transduction efficiency of organoids when used in the AAV9 vector [74].

Delivery of AAV by intravitreal injections is a safe method, but it often leads to low transduction efficiencies of photoreceptors. A novel injection system using peripapillary intravitreal injection promises to be a safe and efficient alternative to standard intravitreal injections [75]. This, together with recent positive results on retinal-transduction efficiency of newly designed second-generation AAVs, holds hope for the future of AAV-based retinal therapies when combined with intravitreal delivery.

Another type of therapeutic strategies are RNA-based therapies, such as antisense oligonucleotides (AONs), which are becoming popular to treat IRD [76, 77]. AONs are relatively small nucleic acid molecules that target the pre-mRNA or mRNA to modify the splicing process, alter translation or degrade a transcript. Currently, four clinical trials using these molecules are ongoing for *CEP290*- (NCT03913130 and NCT03913143), *USH2A*- (NCT03780257), and *RHO*- (NCT04123626) associated IRD. Retinal organoids have been instrumental to evaluate the efficacy and safety of several AON molecules that modulate splicing to either correct defects introduced by deep-intronic variants in *CEP290* [78, 79] and *ABCA4* [80] or to create shorter proteins with a residual function in *USH2A* [81]. This implementation of retinal organoids will be further discussed in “Splicing studies” section.

Analyses of retinal organoids

The advent of new analytical methods that include and integrate multiple next-generation “omics” technologies is on par with the progress of organoid technology (Fig. 3). This facilitates the extraction of useful information from organoids, or a subpopulation of cells, at different levels of complexity and detail.

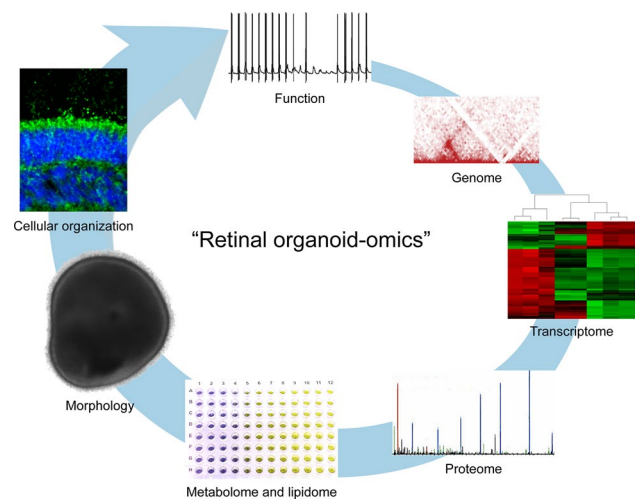


Fig. 3 Retinal organoids can be analysed at multiple levels of complexity such as at gene, protein, metabolome, morphology, cellular and subcellular organizations, and finally—function

Genome analysis

The epigenetic landscape and intragenic/intergenic variants play an important role in regulating gene expression. One such epigenetic feature is a 3D organization of chromatin in the nucleus. The chromatin organization can be examined at a high spatial resolution, using methods such as chromosome conformation capture (3C) assays. In these assays, first the chromatin-deoxyribonucleic acid (DNA) complexes in the nucleus are crosslinked with formaldehyde. Then, the tissue is fragmented, and the DNA is extracted, ligated, and digested with restriction enzymes. Interacting loci are amplified with polymerase chain reaction (PCR) and quantified by sequencing methods [82, 83]. A high-throughput assay called Hi-C allows mapping of chromatin interaction genome-wide in the tissue of interest, in this case, the retina for IRD. For example, the so-called low-input Hi-C analysis of retinal organoids was used to develop the first topologically associated domain (TAD) structure from the human retina and then examine the consequences of an IRD-associated structural variant. This analysis revealed a disrupted chromatin organization with repositioning of domain boundaries, formation of a neo-TAD, and consequent misexpression of *GDPD1* in the RP17 locus of patients with autosomal dominant retinitis pigmentosa (RP) [84]. The low input Hi-C method allows for low amounts of input material and thus mitigates one of the largest hurdles of the retinal organoid system [82], suggesting it could be used to study other IRDs with a genomic reorganisation.

Another promising application of retinal organoids for epigenetic analysis might be chromatin accessibility assay via the transposase-accessible chromatin using sequencing (ATACseq). ATACseq can identify regions of open

chromatin and cell-specific transcription factors binding sites via the action of hyperactive Tn5 transposase and high-throughput deoxyribonucleic acid (DNA) sequencing [85]. It was previously implemented in patient-derived RPE cells to reveal decreased chromatin accessibility in age-related macular degeneration (AMD), which is the most common cause of central vision loss in the elderly [86, 87].

The small size and heterogeneity of cell types in retinal organoids pose significant technical challenges for techniques with higher material demand, lower sensitivity, or difficulty to distinguish between the signal coming from different cell types; this is also true for epigenetic analyses. However, for a disease where a primary tissue is difficult to obtain, such as in IRDs, organoids provide a unique opportunity to study the epigenetic landscape of a specific patient genome in the correct cellular context.

Transcriptome analysis

The retinal organoid system can also be used to quantify the changes in expression levels of retina-specific genes between a patient, or gene-edited line, and control, or following a therapeutic intervention. For this, ribonucleic acid (RNA) is converted into single-strand complementary DNA (cDNA) using a retroviral enzyme, reverse transcriptase with either oligo-dT for priming from the poly-A tails or random hexamers. The cDNA is used as a template for amplification of the gene of interest with PCR [88]. The resulting amplicon is then visualised with an agarose gel electrophoresis in reverse-transcription PCR (RT-PCR), or fluorescence can be incorporated for detection of amplicons during the early exponential phase of the PCR, in so-called quantitative PCR (qPCR) [89]. Pioneering studies used the qPCR technique to show that the temporal profile of neural retinal markers expression of mouse ES-derived organoids follows that of the retina *in vivo* [23]. qPCR is sensitive even for low abundant genes and requires little starting material; therefore, it remains widely used for gene expression analysis in retinal organoids. To detect targets with a very low abundance, droplet digital PCR (ddPCR) can be employed, which is a water–oil emulsion droplet-based method where a sample is split into droplets, and PCR amplification occurs in each individual droplet. This technique was used to quantify the correction of the aberrant splicing in retinal organoids derived from a Leber congenital amaurosis 10 (LCA10) patient post AON treatment [79].

Retinal development mapping

A snapshot of all RNA transcripts can be identified with microarrays or RNA-sequencing (RNA-seq). Microarray analysis utilises a collection of specifically designed short DNA oligos, which gives a quantifiable fluorescent signal

upon hybridization with a cDNA from retinal organoids. With microarray analysis, the rhodopsin-positive cells of D26 and D34 ESC-derived organoids were compared to P12 early postnatal mouse photoreceptors, revealing that D34 were more mature and closer resembling P12 photoreceptors [43]. These arrays are cost-effective and require a small amount of sample material [90].

The array technique allows for transcriptome-wide gene expression profiling, including the ability to detect alternative splicing events, whereas RNA-seq allows for the identification of a larger number of genes than microarrays and is also applicable to unknown transcripts [91]. Here, the cDNA fragments are used for construction of an RNA-seq library, which then is compared to a reference transcriptome after next-generation sequencing. Bulk RNA-seq profiling demonstrated a gradual and continuous increase of photoreceptor-specific genes in developing retinal organoids, with cone-specific markers expressed before rod-specific ones [92]. Also, cone cells were shown to exist at different stages of maturation within a single organoid [93]. RNA-seq was instrumental to confirm that genes related to visual perception, synaptogenesis, and phototransduction increase over time in developing retinal organoids, and their expression is similar to late foetal and adult retinal transcriptomes [34].

The averaged gene expression profiles resulting from the bulk RNA-seq analysis limit its applicability to the mixed cell populations that comprise a retinal organoid. The gene expression profiles of individual cells yielded by single-cell RNA-seq (scRNA-seq), on the other hand, allow expression data to be refined to specific cell types [94]. ScRNA-seq profiling identified photoreceptor populations [95] and also distinguished between rods and cones [96] in mature retinal organoids. scRNA-seq of ten pooled organoids at D220 revealed four major groups of cells: rods, cones, Müller cells, and a mixed population of retinal neurons, including bipolar, retinal ganglion, and amacrine cells [97]. scRNA-seq data from 4 different maturation stages of retinal organoids and bulk RNA-seq of retinal tissue at 16 stages of human retinal development were compared to the mouse transcriptome and revealed species-specific differences of gene expression in specification of cone photoreceptors and horizontal interneurons and gene regulatory networks that pattern the macula [98]. The mature retinal organoid transcriptomes were closer to peripheral than to foveal adult human retina and contain the largest number of diverse cell types at D210–266, and those cell types appear in the following temporal order: ganglion cells, photoreceptor precursors, horizontal cells, amacrine cells, bipolar cells, and Müller cells [11]. Another study used scRNA-seq to show that retinal organoids are similar in cellular composition to the foetal retina at equivalent stages of development; however, differences in levels of gene expression and quality of lamination were observed. Interestingly, lamination was

superior in dissected foetal retina that was cultured under the same conditions as retinal organoids for up to 5 months. The study also described a transition cell population that is situated between progenitor and differentiated cell populations [15]. Furthermore, retinal organoid scRNA-seq has been used to investigate the potential for CRISPR-based genome editing in the retina. Downregulation of genes associated with the homology-directed repair (HDR) pathway (that are crucial for accurate genome editing) after cell division was reported in both adult mouse and human retinas as well as retinal organoid datasets, whereas non-homologous end joining (NHEJ) and microhomology-mediated end joining (MMEJ) pathways were still active, suggesting NHEJ or MMEJ are more likely to be successful than HDR [99]. Nevertheless, despite the power of scRNA-seq the method is continually developing and advances are still needed in read depth, length, and improved sensitivity for the in-depth understanding of gene expression at the single-cell level in organoids.

Isogenic controls

Several studies have compared the expression of a gene of interest in patient-derived organoids versus controls. Organoids derived from a patient with splicing factor-related RP showed differential expression of a number of genes related to ciliary structure and photoreceptor morphology [100]. RNA-seq analysis of patient-derived retinal organoids harbouring mutations in *AIPL1*, underlying severe inherited retinal dystrophy Leber congenital amaurosis type 4 (LCA4), unexpectedly showed no difference in gene expression of *AIPL1* itself or that of other retinal specific genes, but it did of the cortical development gene *NEUROD6* at D25, D60, D88, and D123; furthermore, in the patient-derived organoids, photoreceptors developed normally [101]. In contrast, scRNA-seq of organoids at D100 and D170 bearing a loss of NRL protein confirmed downregulation of rod-specific genes [14].

A gene expression profile of patient-derived retinal organoids can be compared with that of an isogenic control generated by CRISPR/Cas9-mediated correction, thereby reducing inter-individual variation and more precise control of phenotypes associated with a disease-causing mutation. For example, retinal organoids bearing an RP-causative mutation in *RPGR* showed upregulation of necrosis and inflammation receptors when compared to both isogenic and unrelated controls [102]. Similarly, in organoids with a mutation in X-linked juvenile retinoschisis causative gene *RS1*, the expression of *RS1* alongside retinopathy-associated genes *IQCB1* and *OPAI* was reduced compared to isogenic control organoids [103]. Alternatively, an isogenic pair can be created by CRISPR/Cas9-mediated gene knock-out in a healthy control iPSC line. A CRISPR-generated knock-out

of both isoforms of the nuclear hormone receptor thyroid hormone receptor β (Thr β 2 and Thr β 1), but not the Thr β 2 alone, as was previously thought, directed the cone fate specification toward the S-opsin type [12]. The *RP2* gene encodes for a GTPase-activating protein linked to a severe form of X-linked RP. Isogenic disruption of *RP2* in retinal organoids shared expression profile similarities to patient-derived organoids, including upregulation of a number of pro-apoptotic genes compared to isogenic controls that correlated with photoreceptor cell loss [71].

Splicing studies

In the retinal organoid system, RT-PCR and RNA-seq can also enable mapping of developmental switches in splicing and give an insight into the retina-specific alternative splicing events, where several distinct mRNAs are produced from the same gene, leading to different isoforms. Photoreceptors have a high level of alternative splicing with many unique or enriched isoforms. The alternative splicing programme in photoreceptors is independent of *Crx* and it is driven, amongst others, by the protein Musashi-1, which promotes the inclusion of photoreceptor-specific exons [104, 105]. Alternative splicing can also be associated with pathogenic events. For example, the levels of aberrant splicing and pseudoexon inclusion associated with a deep-intronic variant in *CEP290*, which causes LCA10, were higher in patient-derived retinal organoids compared to RPE or other cell types [78]. Retinal organoids were used to show that AONs could correct the aberrant splicing in LCA10 [78, 79] and this approach shows promise in a clinical trial [106].

Mutations can also occur in retinal specific exons; for example, RT-PCR of control retinal organoids showed an increase in expression of the alternatively spliced isoform *REEP6.1*, which harboured a mutation in a family with autosomal recessive RP, correlated with the time course of photoreceptor development [107]. Similarly, expression of a retinal isoform of the ciliopathy and RP-linked gene *DYNC2H1* increased in maturing retinal organoids over time to become the dominant transcript at D200, correlating with the non-syndromic RP in patients with mutations affecting the retinal isoform only [108]. In Stargardt disease, an *ABCA4*-associated progressive disorder of the retina that is initially characterised by a loss of central vision, retinal organoids exhibited enhanced splicing defects, such as pseudoexon insertion caused by deep-intronic variants, compared to transfection of gene constructs in non-retinal cells, and were used to show the therapeutic potential of an AON for splice correction [80]. RNA-seq analysis of *PRPF31* patient organoids revealed changes in alternative splicing of key components involved in the splicing process, as well as part of the microtubule and ciliary networks [100]. CRISPR/Cas9-mediated correction of a *PRPF31* mutation in retinal

organoids and RPE rescued these molecular and cellular defects [100].

To conclude, transcriptome analysis via the RNA-seq method has become a pivotal tool in the analysis of retinal organoid development and disease mechanisms. The disadvantage of RNA-seq is the difficulty in reconstructing full-length transcripts from the assembly of reads, particularly when alternative splicing into highly similar isoforms occurs. Long-read sequencing provides amplification-free, single-molecule sequencing of cDNAs and eliminates the need for the library assembly step, and thus can be more sensitive for the alternative splicing events in distinct cell populations of the retinal organoid [109, 110]. Other limitations of RNA sequencing techniques include sensitivity to the number of reads and underrepresentation of the reads from short and low abundant genes. In addition, a high cost along with a variety of protocols and analysis methods might make RNA-seq techniques challenging to implement.

Proteomic analysis

An increase in RNA transcript numbers does not necessarily lead to an increase in the amount of the encoded protein. RNA or protein stability and post-translational modifications also contribute to protein levels [111, 112]. Western blotting (WB) is an electrophoresis-based protein detection technique that utilises a polyacrylamide gel matrix for size separation of proteins followed by staining of immobilised antigens on immunoblots by using highly specific antibodies [113]. Several studies employed WB to demonstrate a presence of an additional version of a protein, such as TRNT1 [114], decrease of protein expression, such as RS1 [103], and AIPL1 [101] in patient-derived retinal organoids versus control, or rescue of protein expression after treatment [78, 115].

Due to the small size of the laminated retinal organoid, it is challenging to obtain sufficient material for WB analysis. Although one study reports pooling together at least 16 stage-1 (D18-D35) organoids per condition [116], this approach might be even more challenging for later stage organoids due to their small yield, and time- and labour-intensive differentiation protocols to produce sufficient material for robust replicates. A reverse-phase proteomic array (RPPA) that requires nanogram-range amounts of proteins could be implemented to study retinal organoids. In this technique, protein extracts are printed onto nitrocellulose-covered microscope slides and then quantified using antibodies [117].

A more exploratory technique, mass spectrometry (MS) analysis can identify and quantify multiple proteins in complex mixtures by measuring the mass-to-charge ratio of peptides that are labelled with isotopes [118, 119]. For example, MS suggested a role of differential splicing to be more significant in RPE than in organoids [100]. However,

the sensitivity of the MS might be lower in retinal organoids due to its cell population heterogeneity.

Metabolomic analysis

Metabolomics is another -omics approach that allows sensitive and semi-quantitative detection of low molecular weight molecules at a given time. The “metabolome” can rapidly change and reflect the dynamics of a biological system [120]. While metabolomic studies are not very frequent in the area of ophthalmology (recently reviewed in [121] and [122]), they are well-implemented tools for new-born screening and diagnosis of many multisystemic diseases and currently being further developed to find new disease indicators and biomarkers that allow following the progression of a disease or the effect of therapeutic intervention [120]. Using small intestine and pancreas organoids, a study concluded that the organoid system does not recapitulate the full functional metabolomic spectrum of the organ and suggested improvements in the cultivation process [123]. However, the progress in intestinal development has allowed performing metabolic studies in a more robust and reliable manner [124–126]. Unfortunately, this type of study has not yet been fully explored in the retinal organoid field, as shown by the limited literature available.

Imaging techniques, such as hyperspectral imaging (HSPEC), can be used to assess the metabolic activity of the organoids. HSPEC showed that retinol and RA signal intensity increased following an increase in CRX expression. The metabolic state can also be imaged with fluorescence lifetime imaging microscopy (FLIM) that shows glycolytic activity by measuring free and bound NADH distribution. In D150 organoids, the glycolytic region appeared in the laminated outer edge that corresponds to the emergence of a highly metabolically active photoreceptor layer [127]. Recently, a dynamic full-field optical coherence tomography (D-FFOCT) was developed where backscattering from cell dynamics or metabolic activity resulted in higher resolution compared to conventional OCT. This technique could distinguish between RPE and photoreceptor progenitor populations in early-stage organoids [128]. These techniques show promise for the non-invasive determination of the retinal organoid maturation stage; however, it will be important to fully correlate the analysis results with the large array of cell type markers via widely-established immunohistochemical methods.

Interestingly, for retinal organoids, an easy and renewable source of material is the culture medium. Many factors are released to the medium, and they could provide valuable information about the stage of the organoids and the active functions. Furthermore, the used medium is usually discarded and thus the metabolomic studies throughout the complete retinal organoid differentiation could be

established. For example, high-performance liquid chromatography (HPLC) system coupled to MS allowed the analysis of the media content of retinal organoids treated with retinotoxic antibiotic moxifloxacin [129]. Another possibility could be to study the complement system in AMD organoids. In a recent study, the authors performed a quantitative multiplex profiling of all complement components to diagnose disease [130]. Thus, analysing the secretome of AMD organoids using the medium, could provide a correlation with the disease to what has been observed in human biofluids. An alternative targeted method for a specific group of biomarkers could be an enzyme-linked immunosorbent assay (ELISA). This immunoassay can quantitatively measure a marker of interest; however, well-validated and robust antibodies need to be used to ensure reliable measurements [131]. ELISA could be useful to assess the levels of specific components of the complement pathway, as demonstrated recently by a study in plasma of AMD patients [132, 133]. However, the composition of the medium might interfere with the results. For example, if the aim is to study the metabolism of specific amino acid, sugar, protein, or a growth factor if it is already included in the culture medium, it may mask the possible effect. Altogether, exhaustive development might be needed to apply metabolomics as a regular -omics strategy for retinal organoids.

Lipidomic analysis

Lipidomics is another -omics strategy based on measuring the different types of lipids by combining extraction protocols with detection methods such as liquid chromatography-mass spectroscopy. In the past, lipids in the retina of multiple species have been exhaustively studied [134–141]. Depositions of lipids are found in patients suffering from AMD (drusen) or Stargardt disease (lipofuscin). Furthermore, several IRD-linked genes have been associated with lipid metabolism, such as *ELOVL4* and *CERKL*. In addition, sphingolipidosis, such as Gaucher disease, or complex lipid disorders like Sjögren-Larsson syndrome, also present a retinal phenotype. Thus, lipidomics is a very appealing approach to study the mechanism of disease in cellular models. Retinal organoids can be used to study how changes in lipid metabolism affect retinal health; for example, deoxysphinganine-induced photoreceptor apoptosis in retinal organoids, supporting the potential association of serine and lipid metabolism disruption in macular telangiectasia type 2 [142].

Morphological analysis

Most studies of retinal organoids rely on immunohistochemistry (IHC) as a gold standard for characterisation of differentiation and identification of protein and cellular changes

[143]. This microscopy-based technique visualises protein expression and localization by antibody staining. First, a cross-linking fixative, such as paraformaldehyde, is used to preserve the cellular architecture and to immobilise target antigens. The fixation agent can degrade or mask an antigen or epitope of interest; therefore, the optimal fixation and staining conditions should be experimentally determined for each antigen–antibody combination separately. Subsequently, the organoids are cryopreserved with sucrose or similar substance, then embedded in suitable media such as OCT, frozen, and sectioned to obtain thin slices that are eventually subjected to antibody staining. Perpendicular sectioning and careful positioning of the organoids is required to capture the photoreceptors in the correct orientation. A list of commonly used antibodies is provided in Table 2.

IHC can also be adapted for quantitative analysis; for example, the survival of cells in ONL in retinal organoids can be measured, either as cell counts or ONL thickness. This method was used to show photoreceptor degeneration in the ONL of retinal organoids derived from a patient with a mutation in *RP2* and CRISPR-mediated *RP2* knock-out. The cell death also coincided with an increase in apoptotic cells visualised by a TUNEL assay where the 3' ends of the fragmented DNA are labelled with fluorescently tagged dUTP nucleotides. Significantly more TUNEL-positive cells were present in the ONL at D150 in the patient and knock-out organoids compared to the control which pinpointed a peak in photoreceptor cell death, with subsequent thinning of the ONL, by D180 [71].

While severe photoreceptor layer abnormalities or large cysts are visible under bright field microscopy [103], this technique cannot resolve deep into the tissue. Similarly, the IHC method requires sectioning of the organoid, which proves challenging when the intricate 3D structure and interplay between cell layers are of interest. Multi-photon microscopy improves the image quality deeper into the tissue without the need for sectioning. It confines the emitted fluorescence to a small area by combining the multiple low-energy excitation photons precisely in time and space [145]. The use of multi-photon microscopy allows for live imaging of the invagination process in the forming retinal organoid [23], revealed an interkinetic nuclear migration of retinal progenitors in the D20 optic-vesicle epithelium [24], and showed the differences in M/L-opsin and the rhodopsin marker distribution on the surface of mature organoids [10]. Another method of in-depth imaging, light-sheet fluorescence microscopy, illuminates the sample perpendicular to the objective lens with a thin sheet of excitation light, ensuring that the emitted signal arises only from the in-focus regions [146]. Light-sheet fluorescence microscopy helped visualise the ribbon synapse network formed by photoreceptors and bipolar cells alongside the morphology of photoreceptor basal body and inner segments [147]. A major

Table 2 A wide range of antibodies is available for IHC of retinal organoids

Antibody (antigen)	Usage	Host	Supplier	Catalog number	Dilution	References
ABCA4	IRD-causative gene OS protein	Mouse	Rockland Immunochemicals	200301D05	1/100	[11]
Acetylated tubulin	Cilia, inner segment, stages 2,3	Mouse	Sigma-Aldrich	T7451	1/1000	[150]
AP2 α	Neural crest marker, stage 1	Mouse	DSHB	3B5	1/35-1/100	[101, 150]
AP2 α	Neural crest marker, stage 1	Mouse	Santa Cruz Biotechnology	sc12726	1/100-1/200	[32]
AQP1	Cilia, inner segment, stages 2,3	Rabbit	Millipore	ab2219	1/500	[182]
ARL13B	Cilia, inner segment, stages 2,3	Rabbit	Protein Tech	11,711	1/200-1/1000	[10, 11, 101, 182]
ARL13B	Cilia, inner segment, stages 2,3	Mouse	Abcam	ab136648	1/1000	[71]
ARR3	Cone photoreceptor, stage 3	Rabbit	LS Bio	LSC368677	1/300	[10]
ARR3	Cone photoreceptor, stage 3	Goat	Novus Biologicals	NBP137003	1/200	[10, 11]
ARR3	Cone photoreceptor, stage 3	Rabbit	Novus Biologicals	NBP241249	1/1000	[101]
ARR3	Cone photoreceptor, stage 3	Goat	Santa Cruz Biotechnology	sc54355	1/50	[173]
Bassoon	Synapse protein, stage 3	Rabbit	Cell Signalling Technology	6897S	1/200	[34]
Bassoon	Synapse protein, stage 3	Mouse	StressGen	PS003	1/100-1/200	[31, 32]
Bassoon	Synapse protein, stage 3	Mouse	Enzo	SAP7F407	1/500–1/800	[11, 71]
BEST1	RPE	Rabbit	Abcam	ab2182	1/250	[160]
BEST1	RPE	Mouse	Novus Biologicals	NB300164	1/1000	[150]
BiP	Endoplasmic reticulum chaperone	Rabbit	Abcam	ab21685	1/1000	[160]
BrdU	Proliferation marker, S phase, retinal progenitor cells, stage 1	Rat	Accurate	OBT0030	1/250	[144]
BRN3A	RGC, stages 1,2	Mouse	Millipore	ab1585	1/200-1/250	[34, 150, 160, 182]
BRN3B	RGC, stages 1,2	Goat	Santa Cruz Biotechnology	sc31989	1/50	[72]
Calbindin D-28K	Horizontal or amacrine cells	Rabbit	Millipore	ab1778	1/200-1/300	[31, 32]
Calbindin D-28K	Horizontal or amacrine cells	Rabbit	SWANT	CB38	1/500	[101]
Calbindin D-28K	Horizontal or amacrine cells	Rabbit	Calbiochem	PC253L	1/500	[34, 182]
CaR	Amacrine cells and RGC, stage 1	Rabbit	Millipore	ab5054BD	1/500	[10]
CaR	Amacrine cells and RGC, stage 1	Rabbit	SWANT	CR7697	1/500	[101]
CD73	Surface antigen, photoreceptors, stage 2	Mouse	BioLegend	AD2/344002	1/100	[50, 150]
CD73-FIT	Surface antigen, photoreceptors, stage 2	Mouse	BioLegend	AD2/344015	1/1000	[50]
CHAT	Starburst amacrine cells, stage 1	Mouse	Millipore	ab144P	1/100-1/300	[10, 11]

Table 2 (continued)

Antibody (antigen)	Usage	Host	Supplier	Catalog number	Dilution	References
CRALBP	Müller glia, stages 2,3	Mouse	Abcam	ab15051	1/250-1/500	[10, 11, 34, 72, 101, 173, 182]
CRALBP	Müller glia, stages 2,3	Mouse	Invitrogen	MA1813	1/300	[71]
CRX	Photoreceptor progenitors, stages 1,2	Rabbit	GeneTex	GTX124188	1/1000	[144]
CRX	Photoreceptor progenitors, stages 1,2	Mouse	Abnova	H00001406M02	1/100-1/5000	[10, 31, 50, 101, 150]
CRX	Photoreceptor progenitors, stage 1,2	Rabbit	Atlas Antibodies	HPA036763	Jan-50	[160]
CTBP2	Ribbon synapse, Stage 3	n/a	BD Biosciences	612,044	1/300	[10]
EZRIN	Pigment epithelial cells	Rabbit	Cell Signalling Technology	3145S	1/200	[173]
EZRIN	Pigment epithelial cells	Mouse	Sigma-Aldrich	MS661	1/250-1/500	[150, 182]
G0 α	Rod and cone ON bipolar cells, stage 3	n/a	Millipore	Mab3073	1/700	[10]
GNAT1	Rod photoreceptors, stage 3	n/a	GeneTex	GTX114440	1/500	[72]
GT335	Cilia, inner segment, stages 2,3	Mouse	Adipogen Life Sciences	AG20B0020	1/800	[71]
HuC/D	Amacrine cells and RGC, stages 2,3	Mouse	Molecular Probes	a21271	1/200	[31, 32] [144]
Islet1/2	RGC, stages 1,2	Rabbit	Santa Cruz Biotechnology	sc30200	1/200	[31]
KDEL	Endoplasmic reticulum marker	Mouse	Abcam	ab176333	1/500	[160]
Ki67	Proliferation marker, G1, S, G2, and M phase, retinal progenitor cells, stage 1	Mouse	BD Biosciences	550,609	1/200-1/500	[50], [144]
Ki67	Proliferation marker, G1, S, G2, and M phase, retinal progenitor cells, stage 1	Rabbit	Abcam	ab15580	1/100-1/500	[10, 31, 32, 50]
LAMP2	Lysosomal marker	Mouse	Santa Cruz Biotechnology	sc18822	1/50	[173]
LHX2	Retinal progenitor cells, stage 1	Mouse	Santa Cruz Biotechnology	sc81311	1/100	[150]
Meis1/2	Retinal progenitors, stages 1, 2	Goat	Santa Cruz Biotechnology	sc10599	1/200	[144]
MITF	RPE	Mouse	Abcam	ab80651	1/500	[182]
MITF	RPE	Mouse	DAKO	M3621	1/200	[150]
MITF	RPE	Mouse	Exalpha Biologicals	X1405M	1/500	[173]
MITF	RPE	Goat	Exalpha Biologicals	X2398M	1/400	[11]
NES	Neuronal and glial surface marker	Mouse	Abcam	ab22035	1/200	[71]
NES	Retinal progenitors, stage 1	Goat	Sigma-Aldrich	N5413	1/200	[11]
NeuN	Retinal progenitors, stage 1	Mouse	Millipore	Mab377	1/500	[101]
NR2E3	Rod progenitors, stage 2	Mouse	Abcam	ab172542	1/300	[10]
NRL	Rod progenitors, stages 1,2	Goat	R&D Systems	af2945	1/200-1/300	[10, 11, 101]

Table 2 (continued)

Antibody (antigen)	Usage	Host	Supplier	Catalog number	Dilution	References
NRL	Rod progenitors, stage 1,2	Goat	Santa Cruz Biotechnology	sc10971	1/50	[11]
Opsin	Opsin, stage 3	Mouse	Sigma-Aldrich	O4886	1/400	[31]
OPN1SW	Opsin blue, stage 3	Rabbit	Millipore	ab5407	1/200-1/500	[10, 31, 50, 101, 150]
OPN1SW	Opsin blue, stage 3	Goat	Santa Cruz Biotechnology	sc14363	1/150-1/200	[11, 34, 72, 173, 182]
OPN1LW/MW	Opsin red/green, stage 3	Rabbit	Millipore	AB5405	1/200-1/500	[10, 11, 31, 32, 34, 50, 101, 182]
OTX2	Photoreceptor, bipolar, and horizontal cell progenitors, stage 1	Goat	R&D Systems	af1979	1/20-1/500	[101], [144]
OTX2	Photoreceptor, bipolar, and horizontal cell progenitors, stage 1	Rabbit	Millipore	ab9566	1/2000	[150]
PAX6	Photoreceptor, glial, amacrine and horizontal cells progenitors, stage 1	Rabbit	Biologend	901,301	1/300	[144]
PAX6	Photoreceptor, glial, amacrine and horizontal cells progenitors, stage 1	Rabbit	Millipore	ab2237	1/1000	[50, 150]
PAX6	Photoreceptor, glial, amacrine and horizontal cells progenitors, stage 1	Rabbit	Covance	PRB278	1/00-1/300	[31]
PAX6	Photoreceptor, glial, amacrine and horizontal cells progenitors, stage 1	Mouse	Santa Cruz Biotechnology	sc53108	1/200	[116]
PCTN	Basal bodies, staged 2,3	Rabbit	Abcam	ab4448	1/500	[182]
PDE6a	IRD-causative gene	Rabbit	Abcam	ab5659	1/1000	[101]
PCN	Cilia, inner segment, stages 2,3	Mouse	Abcam	ab28144	1/500	[10]
PKC α	Bipolar cells, stages 2,3	Mouse	BD Biosciences	610,107/8	1/100-1/200	[11, 32]
PKC α	Bipolar cells, stages 2,3	Rabbit	Abcam	ab32376	1/200	[11, 71]
PKC α	Bipolar cells, stages 2,3	Rabbit	Millipore	P4334	1/500-1/1000	[182]
PKC α	Bipolar cells, stages 2,3	Rabbit	Sigma-Aldrich	P4334	1/500-1/2000	[10, 34, 50]
PKC α	Bipolar cells, stages 2,3	Rabbit	Santa Cruz Biotechnology	sc17769	1/2000	[150]
PKC α	Bipolar cells, stages 2,3	Rabbit	Santa Cruz Biotechnology	sc208	1/500	[72, 173]
PKC α	Bipolar cells, stages 2,3	Goat	Santa Cruz Biotechnology	sc208G	1/500	[11]
PMEL17	RPE	Mouse	Novus Biologicals	NBP244520	1/500	[182]
PROX1	Horizontal cells, stages 2,3	Rabbit	Millipore	ab5475	1/1500	[32]
PROX1	Horizontal cells, stages 2,3	Rabbit	Millipore	abN278	Jan-00	[72]
PSD95	Postsynaptic adaptor, photoreceptor, stage 3	Mouse	Millipore	Mab1598	1/200	[31]
PVALB	Postsynaptic adaptor, photoreceptor, stage 3	Rabbit	Sigma-Aldrich	P3088	1/200	[11]
RAX	Photoreceptor progenitors, stages 1,2	Mouse	Santa Cruz Biotechnology	sc271889	1/200	[116]

Table 2 (continued)

Antibody (antigen)	Usage	Host	Supplier	Catalog number	Dilution	References
RAX	Photoreceptor progenitors, stages 1,2	Rabbit	Aviva Systems Biology	ARP31926	1/200	[31]
RAX	Photoreceptor progenitors, stages 1,2	Mouse	Sigma-Aldrich	Sab1405061	1/100	[31]
RB	Retinoblastoma-causative gene	Mouse	BD Biosciences	554,136	1/400	[144]
RB	Retinoblastoma-causative gene	Rabbit	Abcam	ab39689	1/500	[144]
RCVN	Photoreceptor progenitors, stage 2 Photoreceptors, stage 3	Rabbit	Millipore	ab5585	1/200-1/2000	[10, 31, 32, 34, 71, 101, 150, 160, 182], [144]
RHO	Photoreceptors, stage 3	Mouse	Millipore	ab5356	1/1000	[101]
RHO	Photoreceptors, stage 3	Rabbit	Millipore	ab9279	1/250	[150]
RHO	Photoreceptors, stage 3	Mouse	Millipore	MabN15	1/100-1/500	[10, 31, 50, 71]
RHO	Photoreceptors, stage 3	Mouse	Sigma-Aldrich	R5403	1/1000	[11]
RHO	Photoreceptors, stage 3	Mouse	Santa Cruz Biotechnology	sc57432	1/200	[31, 32, 72, 173]
RIBEYE	Ribbon synapse, stage 3	Rabbit	Synaptic Systems	192,103	1/800	[11]
RIBEYE	Ribbon synapse, stage 3	Mouse	BD Bioscience	612,044	1/100-1/500	[32, 50]
ROM1	OS, stage 3	Rabbit	ProteinTech	219841AP	1/200	[173]
RP2	IRD-causative gene and plasma membrane/basal body	Rabbit	ProteinTech	141511AP	1/200	[71]
RPE65	Pigment epithelial cells	Mouse	Abcam	ab78036	1/100	[173]
SOX9	Photoreceptor progenitors, stage 1	Mouse	Millipore	ab5535	1/1000	[150]
Synaptophysin	Photoreceptor progenitors, stage 1	Mouse	Sigma-Aldrich	S5768	1/100	[31]
Syntaxin	Outer plexiform layer marker	Mouse	Sigma-Aldrich	S0664	1/200	[31]
TOM20	Mitochondria	Mouse	Santa Cruz Biotechnology	sc17764	1/150	[71]
TOMM20	Mitochondria	Mouse	Abcam	ab56783	1/400	[11]
TRPM1	ON bipolar cells	Rabbit	Atlas Antibodies	HPA014779	1/200	[11]
TUBB3	Cytoskeletal marker, RGC, stage 2	Mouse	Covance	MMS435P	1/800	[31]
TUBB3	Cytoskeletal marker, RGC, stage 2	Mouse	Neuromics	MO15013	1/500	[101]
VGLUT	Postsynaptic marker, photoreceptor terminals, stage 3	Guinea Pig	Millipore	ab5905	1/2000	[10]
Vimentin	Müller glia, stages 2,3	Rabbit	Abcam	ab92547	1/400	[32]
VSX2	Retinal progenitors or bipolar cells, stages 1, 2	Rabbit	Sigma-Aldrich	a96476	1/200	[144]
VSX2	Retinal progenitors or bipolar cells, stages 1, 2	Sheep	Abcam	ab16142	1/200-1/500	[34, 182]
VSX2	Retinal progenitors or bipolar cells, stages 1, 2	Rabbit	Sigma-Aldrich	HPA003436	1/50–1/200	[31, 32]

Table 2 (continued)

Antibody (antigen)	Usage	Host	Supplier	Catalog number	Dilution	References
VSX2	Retinal progenitors or bipolar cells, stages 1, 2	Sheep	Exalpha Biologicals	X1179P	1/200	[10]
VSX2	Retinal progenitors or bipolar cells, stages 1, 2	Mouse	Santa Cruz Biotechnology	sc365519	1/2000	[150]
ZO1	RPE	Rabbit	Abcam	ab59720	1/400	[11]
ZO1	RPE	Rabbit	Thermo Fisher Scientific	c617300	1/100	[173]
ZO1	RPE	Goat	Invitrogen	PA519090	1/250	[150]

The table includes a list of antigens, alongside with indication of the target structure or applicability, host species, where it can be purchased, which dilutions it was used at, and reference to the papers the antibody was used in

limitation of the multiphoton imaging of live organoids over longer periods of time is the photodamage to the tissue caused by the excitation light and the need for intrinsic fluorescent markers, potentially necessitating the production of reporter cell lines.

A technique called optical coherence tomography (OCT) allows non-invasive imaging in the eye *in vivo* and can also be applied to organoids to reveal the internal organisation via the difference in light wave reflectance between nuclear and plexiform layers. An appearance of a layer with high reflectance was reported at D150 near the outer laminated edge of the organoid [127] while another group observed the appearance of alternating high and low reflectance layers at approximately the same stage [10].

The depth of imaging with the multiphoton technique is limited by the penetration of the excitation. Clearing is a chemical treatment that equalises the reflection indexes of the cell membranes and cytoplasm, thus minimizing light scattering, and allows light to travel through a thicker tissue while preserving its excitation and emission efficiency. PACT (passive clarity technique) clearing requires organoids to be fixed with paraformaldehyde, and embedded into hydrogel monomer, after which the resulted hydrogel-organoid hybrid is cleared from the membrane's lipids [147, 148]. Alternatively, during the 3DISCO (3D imaging of solvent-cleared organs) procedure, the tissue is dehydrated with increasing concentrations of tetrahydrofuran and then impregnated with optical clearing agent dibenzyl ether [149]. The former technique enabled imaging of whole mature organoids at D195 with recoverin, rhodopsin, and cone arrestin staining [150]. During the clearing procedures, the tissue is dehydrated or impregnated with a chemical agent. This can cause a heterogeneous tissue expansion or shrinkage, which might disturb tissue organization. However, a homogeneous tissue expansion of the organoid has the potential to provide a higher resolution imaging of some organelles through expansion microscopy. Second,

the stringent chemical treatment might disturb specific antigens on the cleared tissue, limiting the number of useful antibodies. Furthermore, intact organoid clearing requires one specimen per stain which is demanding on production and replicates.

Some potential future applications, such as high throughput testing of drugs or gene therapies, demand an increase in the analysis speed and screening capacity. With an estimated capacity of 200,000 samples per day, a 3D automated reporter quantification (3D-ARQ) platform combines a microplate reader and an excitation/emission detection for the quantitative screening of retinal organoids stained with fluorescent dyes, for example Calcein AM dye that accumulates in the cytoplasm of live cells and is used in viability assays, or JC-1 that allows visualization of the mitochondria rich inner segments of photoreceptors [151].

Often, the subcellular structures of the organoids are of interest, for example, the organization of the membranes inside the OS of photoreceptors, or the structure of the cilium. Light microscopy cannot resolve subcellular structures due to the limited resolving power, whereas transmission electron microscopy (TEM) utilises electrons instead of light and can achieve resolution well below 1 nm. However, it requires elaborate sample preparation with the organoid section undergoing fixation, dehydration, and resin embedding. Imaging with TEM revealed photoreceptor-characteristic organisation and structures, such as the mitochondria rich inner segment, connecting cilium, basal bodies, adherens junctions at the OLM, and microvilli along with membranous disks inside immature OS [10, 17, 26, 71, 78, 129, 152]. TEM imaging also showed the emergence of a ribbon synapse between photoreceptors and bipolar cells in the inner plexiform layer which suggests the functional maturation of retinal organoids [10, 16, 26, 153]. Correlative light and electron microscopy (CLEM) can be used to study the same regions of cells by both light microscopy and TEM and has been used to study retinal organoids to provide

ultrastructural information, as well as antigen localisation by immuno-EM [154]. Overall, microscopy is a widely used technique for retinal organoid analysis as it provides an insight into their morphological, molecular, and, to some extent, functional properties.

Functional analysis

Light responsiveness and synaptic transmission are two crucial features of the functional maturation of photoreceptors and the retina. The light response of a cell can be accessed by measuring a change in its ionic currents in response to light using a patch-clamp. With the patch-clamp, the glass micropipette filled with an electrolytic solution serves as a recording electrode. The electrode touches the membrane of the cell and the suction is applied to establish a tight contact between the pipette and the membrane. This forces the flow of ionic current across the sealed patch of the cell membrane to enter the pipette [155, 156]. Photoreceptor cells may also be stimulated by chemicals, such as cGMP, a secondary messenger in the phototransduction cascade, that potentially mimics the dark current, non-excited state of photoreceptors [157]. In early development, the neurotransmitter GABA is depolarizing and later in development becomes inhibitory; thus the response to it indicates emerging of a functional neuronal network [158]. The patch-clamp recording of recoverin-positive cells in D100 organoids, recorded elevated resting potential and current when compared to control cells, and also the outward current was suppressed with tetraethylammonium, signifying a current that is consistent with photoreceptor electrophysiology [159]. Another study showed that in single and pooled organoids at D150, the response to light, cGMP, and GABA stimulation of RGCs was similar to the developing retina. These experiments require the addition of 9 or 11-*cis* retinal, a chromophore essential for rhodopsin activity, which also serves as a control for the response being opsin-mediated [17]. The OS containing cells of retinal organoids were reported to be comparable to rods of mice retina before eye-opening in their membrane capacity, potential, and resistance recordings. A whole-cell recording of presumed photoreceptors seemed to exhibit detectable hyperpolarization-activated current and the current/voltage curve resembles that of rods [102]. Although the patch-clamp technique is limited by low experimental throughput, it has an important advantage of recording a photoreceptor-specific signal.

Another method to investigate the functionality of retinal organoids utilises confocal or multi-photon microscopy to measure changes in intracellular Ca^{2+} indicative of the inward dark current that is characteristic of photoreceptors. The fluorescent calcium dye Fura-2 allows for visualization of the increase Ca^{2+} influx in response to cGMP-analogue in cells of D45 and D90 [31], D175 [150], and in

cell surface antigen CD73-positive photoreceptors of D190 retinal organoids [50]. In cells of retinal organoids that were genetically modified to express the fluorescent calcium sensor GCaMP6s, a change in Ca^{2+} influx in response to light stimulation was recorded in photoreceptors and in OFF bipolar cells but very few ON bipolar cells [11].

Two-photon microscopy has been combined with patch-clamp electrophysiological recordings to test membrane localization and functionality of optogenetic constructs in retinal organoids. Several types of light-sensitive microbial opsins were expressed in cells of the retinal organoids and excitatory photocurrents were observed for the depolarizing opsins alongside inhibitory photocurrents for the hyperpolarizing opsins [160].

Micro-electrode arrays (MEAs) contain multiple electrodes embedded into a ceramic or glass carrier [161]. Retinal organoids are placed with RGCs facing down onto the MEA and a light or chemical stimulus is applied, resulting in detectable voltage changes [162]. A stronger response to light was observed in control compared to AMD patient-derived organoids [129]. A comparison between the recording of D150 organoids derived control versus a patient with a mutation in *PRPF31*, causing the degeneration of the mid-peripheral retina, implied a significantly reduced response to GABA, but no changes in response to cGMP-analogue [100]. The advantage of the MEA technique is that it measures output from the RGCs which shows inner retinal connectivity; however, the MEA has the challenge of being reliant on the presence of both mature RGCs and photoreceptors at the same stage. This is challenging given the reduction in RGCs by the stage that photoreceptors have developed, as well as the necessity to preserve an inner retinal structure and OS while setting up the MEA. Furthermore, for the MEA, extra care should be taken with the experimental design to eliminate the other sources of electrical signal other than photoreceptors, unlike Ca^{2+} imaging or patch clamping where the origin of the response is more clearly identified.

An important potential addition to testing photoreceptor-driven responses would be to generate a disruption of the elements of the phototransduction pathway, such as by CRISPR/Cas9-mediated knock-out, to confirm the source of the responses. While testing the light responsiveness of retinal organoids *in vitro* is a “holy grail” of organoid characterisation, there is still a lot of work to be done before it could be used as a routine and reproducible measure of photoreceptor function in disease or following rescue.

Limitations of retinal organoids as models of the *in vivo* retina

In the retina, the OS of cone and rod photoreceptors are specialised primary cilia that contain stacks of deep membrane

folds of the plasma membrane, or double-membrane disks enclosed by the plasma membrane, respectively [8]. The structure of these disks is important for phototransduction, as they harbour light-sensitive opsins that are conjugated with the chromophore 11-*cis*-retinal. A major challenge in retinal organoid technology to study photoreceptor disease has been to produce properly stacked OS. Mature retinal organoids contain OS-like structures containing membranous disks that are loaded with opsins [154], but lack the correct disk stacking and orientation. Moreover, an extensive characterisation of the observed membranous structures remains to be done [17, 26, 27, 78, 150, 163]. Notwithstanding, retinal organoids can still be instrumental in studying disk and OS biogenesis [19].

OS membrane disks are renewed and shed daily [164, 165]. When shed, they are phagocytosed by the RPE cells [166]. The RPE supports the high metabolic rate of the photoreceptors by allowing the flow of nutrients from the choroid [167] and participates in the visual cycle by creating ionic gradients and converting all-*trans*-retinal into 11-*cis*-retinal [168, 169]. During development, the RPE secretes compounds required for photoreceptor maturation [30, 170–172]. Retinal organoids usually contain RPE; however, they are generally juxtaposed to the photoreceptors in a clump, and not in a monolayer like the situation *in vivo*. Therefore, the challenge remains to generate an optic cup-like structure where RPE and retina co-exist in close proximity. A recently developed retina-on-a-chip microfluidic device reported such a co-culture by the embedding of the retinal organoid in hydrogel within a small distance of RPE for 7 days, but there was only a small region of contact between the three-dimensional organoids and the two-dimensional RPE [173].

Another structure yet to be replicated is the fovea, a substructure in the centre of the human retina that is required for high-acuity colour vision. The absence of rod photoreceptors and other retinal cell types in the foveal pit allows light to directly stimulate densely packed cones. The fovea is specific to human and non-human primates and is selectively affected by diseases such as macular degeneration. The fovea develops postnatally in the area of the retina where the development of rods from late retinal progenitor cells is inhibited, and the location of this area is likely to be determined by transcription factors involved in the definition of the axis of the retina [174]. While the spontaneous induction of the foveal pit might not be likely in the organoid, several studies reported the generation of cone-enriched organoids, possibly by removal of rod-favouring RA [97, 175, 176].

Blood vessel and immune-related cells are also missing from retinal organoids; these are derived from the mesoderm and during development migrate into the developing optic vesicles. The addition of these cells to retinal organoids would likely require assembloid type technology to bring

together cells from different developmental lineages, which was pioneered in brain organoids [177]. Recently, a model of outer-blood-retinal barrier on-a-chip has been described combining RPE and endothelial cells in a microfluidic chamber [178].

Future outlook

The small size and inherent heterogeneity of cell types in retinal organoids pose significant technical challenges for the types of analysis with higher material demand, lower sensitivity, or difficulty to distinguish between the signal coming from different cell types. It is, however, important to realise the potential of the retinal organoids to reveal neuroretina-specific gene regulation, pathological processes, and therapeutic manipulation.

It would be desirable to increase the efficiency and reproducibility of organoid production and decrease the labour required for their production. To do so, first, it is important to understand the reasons for the innate heterogeneity between iPSC lines and why some lines generate organoids more efficiently than others. More reproducible organoid generation from a particular cell line can be achieved by a better understanding of epigenetic control of iPSC pluripotency [179], as well as the neurodevelopmental factors that are involved in neural patterning and cell fate decisions. To improve and accelerate differentiations, organoids may be grown in rotating-wall vessel bioreactors [153, 180]. Also, reduction of the required labour and level of manual skill is desirable. For this, scraping or checkerboard methods that bypass the manual dissection step to help increase the yield of NRVs obtained are potentially useful [181, 182]. One such example, the recently described AMASS (agarose microwell array seeding and scraping), combines a controlled number of cells seeding in a microwell array with a checkerboard scraping. With this method, more than 3000 organoids were obtained in a single well of a 6-well plate [11]. Culture conditions could also mimic physiological conditions better through assembloid methodologies, such as combining cultures of the tissues produced independently to improve cell cross-talk and implement the use of biomaterials for cellular support [177, 183]. Current state-of-the-art differentiation protocols span several months and up to a year, for a fully mature retinal organoid. Organoid or precursor freezing might help address this and facilitate collaborations across laboratories in the field [150]. Ideally, retinal organoids could be shipped at room temperature at any stage for at least 5 days and still maintain their biological activity and functionality [184]. The heterogeneity of the retinal organoid samples should also be considered regarding analyses that are focused on certain cell types. As retinal organoids are small, the cell type of interest

might be underrepresented and the useful signal lost due to the noise in individual organoids. It can be enriched by manual dissection [185], by coupling MS with flow cytometry, or via fluorescent reporters [43, 50, 92]. In addition, another way of specific cell-type enrichment would be to minimise the material needed for some procedures by refining their specificity and the signal-to-noise ratio.

In conclusion, we now have a number of state-of-the-art techniques that can facilitate analysis of the retinal organoids at different levels of complexity to understand disease mechanisms and test potential therapies. An expansion of the analytical toolbox will increase the benefit of the retinal organoid model for teasing apart the molecular mechanism of genetic blinding diseases.

Acknowledgements The authors would like to thank Dr. Giuliana Gagliardi for comments and advice on the manuscript.

Author contributions TAVA and JCS produced initial drafts of the manuscript, tables, and figures. RR, AG, RWJC and MEC conceived the idea and edited the manuscript, figures and table drafts. All authors edited and approved the manuscript to be submitted.

Funding The authors are supported by ZonMW (TOP Grant number 9121 6051 to RR and RWJC), the Foundation Fighting Blindness USA (FFB-PPA-0717RAD to AG and RWJC, and FFB-PPA-1719-RAD to RR and MEC), and the Proefdiervrij project support to TAVA. RR and RWJC are also supported by the Landelijke Stichting voor Blinden en Slechtienden, Stichting Retina Nederland Fonds, Stichting Beheer Het Schild, Stichting Blinden-Penning, and Stichting Steunfonds Uitzicht via Uitzicht 2016/2017-22, together with the Gelderse Blindenstichting, Rotterdamse Stichting Blindenbelangen, Stichting tot Verbetering van het Lot der Blinden ‘Het Lot’, and Stichting voor gehandicapte kinderen Dowilvo. AG is supported by the Landelijke Stichting voor Blinden en Slechtienden and Stichting Oogfonds via Uitzicht 2019-17, together with Stichting Blindenhulp, Rotterdamse Stichting Blindenbelangen and Dowilvo. Fight for Sight UK and the Wellcome Trust to MEC. The funding organizations had no role in the design or conduct of this review. They provided unrestricted grants.

Availability of data and materials Not applicable.

Declarations

Conflict of interest The authors declare that they have no conflict of interest.

Ethics approval and consent to participate Not applicable.

Consent for publication Not applicable.

Open Access This article is licensed under a Creative Commons Attribution 4.0 International License, which permits use, sharing, adaptation, distribution and reproduction in any medium or format, as long as you give appropriate credit to the original author(s) and the source, provide a link to the Creative Commons licence, and indicate if changes were made. The images or other third party material in this article are included in the article's Creative Commons licence, unless indicated otherwise in a credit line to the material. If material is not included in the article's Creative Commons licence and your intended use is not

permitted by statutory regulation or exceeds the permitted use, you will need to obtain permission directly from the copyright holder. To view a copy of this licence, visit <http://creativecommons.org/licenses/by/4.0/>.

References

1. www.sph.uth.tmc.edu/RetNet/ R
2. Acland GM, Aguirre GD, Ray J, Zhang Q, Aleman TS, Cideciyan AV, Pearce-Kelling SE, Anand V, Zeng Y, Maguire AM, Jacobson SG, Hauswirth WW, Bennett J (2001) Gene therapy restores vision in a canine model of childhood blindness. *Nat Genet* 28:92–95. <https://doi.org/10.1038/ng0501-92>
3. Bainbridge JW, Mehat MS, Sundaram V, Robbie SJ, Barker SE, Ripamonti C, Georgiades A, Mowat FM, Beattie SG, Gardner PJ, Feathers KL, Luong VA, Yzer S, Balaggan K, Viswanathan A, de Ravel TJ, Casteels I, Holder GE, Tyler N, Fitzke FW, Weleber RG, Nardini M, Moore AT, Thompson DA, Petersen-Jones SM, Michaelides M, van den Born LI, Stockman A, Smith AJ, Rubin G, Ali RR (2015) Long-term effect of gene therapy on Leber's congenital amaurosis. *N Engl J Med* 372:1887–1897. <https://doi.org/10.1056/NEJMoa1414221>
4. Bennett J, Wellman J, Marshall KA, McCague S, Ashtari M, DiStefano-Pappas J, Elci OU, Chung DC, Sun J, Wright JF, Cross DR, Aravand P, Cyckowski LL, Bennicelli JL, Mingozzi F, Auricchio A, Pierce EA, Ruggiero J, Leroy BP, Simonelli F, High KA, Maguire AM (2016) Safety and durability of effect of contralateral-eye administration of AAV2 gene therapy in patients with childhood-onset blindness caused by RPE65 mutations: a follow-on phase 1 trial. *The Lancet* 388:661–672. [https://doi.org/10.1016/s0140-6736\(16\)30371-3](https://doi.org/10.1016/s0140-6736(16)30371-3)
5. Slijkerman RW, Song F, Astuti GD, Huynen MA, van Wijk E, Stieger K, Collin RW (2015) The pros and cons of vertebrate animal models for functional and therapeutic research on inherited retinal dystrophies. *Prog Retin Eye Res* 48:137–159. <https://doi.org/10.1016/j.preteyeres.2015.04.004>
6. Lynn SA, Keeling E, Dewing JM, Johnston DA, Page A, Cree AJ, Tumbarello DA, Newman TA, Lotery AJ, Ratnayaka JA (2018) A convenient protocol for establishing a human cell culture model of the outer retina. *F1000Research* 7:1107–1107. <https://doi.org/10.12688/f1000research.15409.1>
7. Takahashi K, Tanabe K, Ohnuki M, Narita M, Ichisaka T, Tomoda K, Yamanaka S (2007) Induction of pluripotent stem cells from adult human fibroblasts by defined factors. *Cell* 131:861–872. <https://doi.org/10.1016/j.cell.2007.11.019>
8. Sung CH, Chuang JZ (2010) The cell biology of vision. *J Cell Biol* 190:953–963. <https://doi.org/10.1083/jcb.201006020>
9. Graw J (2010) Eye development. *Curr Top Dev Biol* 90:343–386. [https://doi.org/10.1016/s0070-2153\(10\)90010-0](https://doi.org/10.1016/s0070-2153(10)90010-0)
10. Capowski EE, Samimi K, Mayerl SJ, Phillips MJ, Pinilla I, Howden SE, Saha J, Jansen AD, Edwards KL, Jager LD, Barlow K, Valiauga R, Erlichman Z, Hagstrom A, Sinha D, Sluch VM, Chamling X, Zack DJ, Skala MC, Gamm DM (2019) Reproducibility and staging of 3D human retinal organoids across multiple pluripotent stem cell lines. *Development*. <https://doi.org/10.1242/dev.171686>
11. Cowan CS, Renner M, De Gennaro M, Gross-Scherf B, Goldblum D, Hou Y, Munz M, Rodrigues TM, Krol J, Szikra T, Cuttat R, Waldt A, Papasaikas P, Diggelmann R, Patino-Alvarez CP, Galliker P, Spirig SE, Pavlinic D, Gerber-Hollbach N, Schuierer S, Srdanovic A, Balogh M, Panero R, Kusnyerik A, Szabo A, Stadler MB, Orgül S, Picelli S, Hasler PW, Hierlemann A, Scholl HPN, Roma G, Nigsch F, Roska B (2020) Cell types of

- the human retina and its organoids at single-cell resolution. *Cell* 182:1623–1640.e34. <https://doi.org/10.1016/j.cell.2020.08.013>
12. Eldred KC, Hadyniak SE, Hussey KA, Brennerman B, Zhang P-W, Chamling X, Sluch VM, Welsbie DS, Hattar S, Taylor J, Wahlin K, Zack DJ, Johnston RJ (2018) Thyroid hormone signaling specifies cone subtypes in human retinal organoids. *Science*. <https://doi.org/10.1126/science.aau6348>
 13. Fligor CM, Langer KB, Sridhar A, Ren Y, Shields PK, Edler MC, Ohlemacher SK, Sluch VM, Zack DJ, Zhang C, Suter DM, Meyer JS (2018) Three-dimensional retinal organoids facilitate the investigation of retinal ganglion cell development, organization and neurite outgrowth from human pluripotent stem cells. *Sci Rep* 8:14520. <https://doi.org/10.1038/s41598-018-32871-8>
 14. Kallman A, Capowski EE, Wang J, Kaushik AM, Jansen AD, Edwards KL, Chen L, Berlinicke CA, Joseph Phillips M, Pierce EA, Qian J, Wang TH, Gamm DM, Zack DJ (2020) Investigating cone photoreceptor development using patient-derived NRL null retinal organoids. *Commun Biol* 3:82. <https://doi.org/10.1038/s42003-020-0808-5>
 15. Sridhar A, Hoshino A, Finkbeiner CR, Chitsazan A, Dai L, Haugan AK, Eschenbacher KM, Jackson DL, Trapnell C, Birmingham-McDonogh O, Glass I, Reh TA (2020) Single-cell transcriptomic comparison of human fetal retina, hPSC-derived retinal organoids, and long-term retinal cultures. *Cell Rep* 30(1644–1659):e4. <https://doi.org/10.1016/j.celrep.2020.01.007>
 16. Wahlin KJ, Maruotti JA, Sripathi SR, Ball J, Angueyra JM, Kim C, Grebe R, Li W, Jones BW, Zack DJ (2017) Photoreceptor outer segment-like structures in long-term 3D retinas from human pluripotent stem cells. *Sci Rep* 7:766. <https://doi.org/10.1038/s41598-017-00774-9>
 17. Zhong X, Gutierrez C, Xue T, Hampton C, Vergara MN, Cao LH, Peters A, Park TS, Zambidis ET, Meyer JS, Gamm DM, Yau KW, Canto-Soler MV (2014) Generation of three-dimensional retinal tissue with functional photoreceptors from human iPSCs. *Nat Commun* 5:4047. <https://doi.org/10.1038/ncomms5047>
 18. Fligor CM, Lavekar SS, Harkin J, Shields PK, VanderWall KB, Huang K-C, Gomes C, Meyer JS (2021) Extension of retinofugal projections in an assembled model of human pluripotent stem cell-derived organoids. *Stem Cell Rep*. <https://doi.org/10.1016/j.stemcr.2021.05.009>
 19. Corral-Serrano JC, Lamers IJC, van Reeuwijk J, Duijkers L, Hoogendoorn ADM, Yildirim A, Argyrou N, Ruigrok RAA, Letteboer SJF, Butcher R, van Essen MD, Sakami S, van Beersum SEC, Palczewski K, Cheatham ME, Liu Q, Boldt K, Wolfrum U, Ueffing M, Garanto A, Roepman R, Collin RWJ (2020) PCARE and WASF3 regulate ciliary F-actin assembly that is required for the initiation of photoreceptor outer segment disk formation. *Proc Natl Acad Sci U S A* 117:9922–9931. <https://doi.org/10.1073/pnas.1903125117>
 20. Lamba DA, Karl MO, Ware CB, Reh TA (2006) Efficient generation of retinal progenitor cells from human embryonic stem cells. *Proc Natl Acad Sci U S A* 103:12769–12774. <https://doi.org/10.1073/pnas.0601990103>
 21. Osakada F, Ikeda H, Mandai M, Wataya T, Watanabe K, Yoshimura N, Akaike A, Sasai Y, Takahashi M (2008) Toward the generation of rod and cone photoreceptors from mouse, monkey and human embryonic stem cells. *Nat Biotechnol* 26:215–224. <https://doi.org/10.1038/nbt1384>
 22. Meyer JS, Shearer RL, Capowski EE, Wright LS, Wallace KA, McMillan EL, Zhang S-C, Gamm DM (2009) Modeling early retinal development with human embryonic and induced pluripotent stem cells. *Proc Natl Acad Sci* 106:16698–16703. <https://doi.org/10.1073/pnas.0905245106>
 23. Eiraku M, Takata N, Ishibashi H, Kawada M, Sakakura E, Okuda S, Sekiguchi K, Adachi T, Sasai Y (2011) Self-organizing optic-cup morphogenesis in three-dimensional culture. *Nature* 472:51–56. <https://doi.org/10.1038/nature09941>
 24. Nakano T, Ando S, Takata N, Kawada M, Muguruma K, Sekiguchi K, Saito K, Yonemura S, Eiraku M, Sasai Y (2012) Self-formation of optic cups and storable stratified neural retina from human ESCs. *Cell Stem Cell* 10:771–785. <https://doi.org/10.1016/j.stem.2012.05.009>
 25. Reichman S, Terray A, Slembrouck A, Nanteau C, Orioux G, Habeler W, Nandrot EF, Sahel JA, Monville C, Goureau O (2014) From confluent human iPSC cells to self-forming neural retina and retinal pigmented epithelium. *Proc Natl Acad Sci U S A* 111:8518–8523. <https://doi.org/10.1073/pnas.1324212111>
 26. Gonzalez-Cordero A, Kruczek K, Naeem A, Fernando M, Kloc M, Ribeiro J, Goh D, Duran Y, Blackford SJI, Abelleira-Hervas L, Sampson RD, Shum IO, Branch MJ, Gardner PJ, Sowden JC, Bainbridge JWB, Smith AJ, West EL, Pearson RA, Ali RR (2017) Recapitulation of human retinal development from human pluripotent stem cells generates transplantable populations of cone photoreceptors. *Stem Cell Rep* 9:820–837. <https://doi.org/10.1016/j.stemcr.2017.07.022>
 27. Lowe A, Harris R, Bhansali P, Cvekl A, Liu W (2016) Intercellular adhesion-dependent cell survival and ROCK-regulated actomyosin-driven forces mediate self-formation of a retinal organoid. *Stem Cell Reports* 6:743–756. <https://doi.org/10.1016/j.stemcr.2016.03.011>
 28. Haynes T, Gutierrez C, Aycinena J-C, Tsonis PA, Del Rio-Tsonis K (2007) BMP signaling mediates stem/progenitor cell-induced retina regeneration. *Proc Natl Acad Sci* 104:20380–20385. <https://doi.org/10.1073/pnas.0708202104>
 29. Huang J, Liu Y, Oltean A, Beebe DC (2015) Bmp4 from the optic vesicle specifies murine retina formation. *Dev Biol* 402:119–126. <https://doi.org/10.1016/j.ydbio.2015.03.006>
 30. Kuwahara A, Ozone C, Nakano T, Saito K, Eiraku M, Sasai Y (2015) Generation of a ciliary margin-like stem cell niche from self-organizing human retinal tissue. *Nat Commun* 6:6286. <https://doi.org/10.1038/ncomms7286>
 31. Mellough CB, Collin J, Khazim M, White K, Sernagor E, Steel DH, Lako M (2015) IGF-1 signaling plays an important role in the formation of three-dimensional laminated neural retina and other ocular structures from human embryonic stem cells. *Stem Cells* 33:2416–2430. <https://doi.org/10.1002/stem.2023>
 32. Zerti D, Molina MM, Dorgau B, Mearns S, Bauer R, Al-Aama J, Lako M (2021) IGFBPs mediate IGF-1's functions in retinal lamination and photoreceptor development during pluripotent stem cell differentiation to retinal organoids. *Stem Cells* 39:458–466. <https://doi.org/10.1002/stem.3331>
 33. Chichagova V, Hilgen G, Ghareeb A, Georgiou M, Carter M, Sernagor E, Lako M, Armstrong L (2020) Human iPSC differentiation to retinal organoids in response to IGF1 and BMP4 activation is line- and method-dependent. *Stem Cells* 38:195–201. <https://doi.org/10.1002/stem.3116>
 34. Kaya KD, Chen HY, Brooks MJ, Kelley RA, Shimada H, Nagashima K, de Val N, Drinnan CT, Gieser L, Kruczek K, Erceg S, Li T, Lukovic D, Adlakhia YK, Welby E, Swaroop A (2019) Transcriptome-based molecular staging of human stem cell-derived retinal organoids uncovers accelerated photoreceptor differentiation by 9-cis retinal. *Mol Vis* 25:663–678
 35. Wagstaff PE, ten Asbroek ALMA, ten Brink JB, Jansonius NM, Bergen AAB (2021) An alternative approach to produce versatile retinal organoids with accelerated ganglion cell development. *Sci Rep* 11:1101. <https://doi.org/10.1038/s41598-020-79651-x>
 36. Bartsch U, Oriyakhel W, Kenna PF, Linke S, Richard G, Petrowitz B, Humphries P, Farrar GJ, Ader M (2008) Retinal cells integrate into the outer nuclear layer and differentiate into mature photoreceptors after subretinal transplantation into adult mice.

- Exp Eye Res 86:691–700. <https://doi.org/10.1016/j.exer.2008.01.018>
37. MacLaren RE, Pearson RA, MacNeil A, Douglas RH, Salt TE, Akimoto M, Swaroop A, Sowden JC, Ali RR (2006) Retinal repair by transplantation of photoreceptor precursors. *Nature* 444:203–207. <https://doi.org/10.1038/nature05161>
 38. Santos-Ferreira T, Llonch S, Borsch O, Postel K, Haas J, Ader M (2016) Retinal transplantation of photoreceptors results in donor-host cytoplasmic exchange. *Nat Commun* 7:13028. <https://doi.org/10.1038/ncomms13028>
 39. Singh MS, Balmer J, Barnard AR, Aslam SA, Moralli D, Green CM, Barnea-Cramer A, Duncan I, MacLaren RE (2016) Transplanted photoreceptor precursors transfer proteins to host photoreceptors by a mechanism of cytoplasmic fusion. *Nat Commun* 7:13537. <https://doi.org/10.1038/ncomms13537>
 40. Pearson RA, Gonzalez-Cordero A, West EL, Ribeiro JR, Aghaizu N, Goh D, Sampson RD, Georgiadis A, Waldron PV, Duran Y, Naem A, Kloc M, Cristante E, Kruczek K, Warre-Cornish K, Sowden JC, Smith AJ, Ali RR (2016) Donor and host photoreceptors engage in material transfer following transplantation of post-mitotic photoreceptor precursors. *Nat Commun* 7:13029. <https://doi.org/10.1038/ncomms13029>
 41. Gasparini SJ, Llonch S, Borsch O, Ader M (2019) Transplantation of photoreceptors into the degenerative retina: current state and future perspectives. *Prog Retin Eye Res* 69:1–37. <https://doi.org/10.1016/j.preteyeres.2018.11.001>
 42. Lamba DA, Gust J, Reh TA (2009) Transplantation of human embryonic stem cell-derived photoreceptors restores some visual function in Crx-deficient mice. *Cell Stem Cell* 4:73–79. <https://doi.org/10.1016/j.stem.2008.10.015>
 43. Gonzalez-Cordero A, West EL, Pearson RA, Duran Y, Carvalho LS, Chu CJ, Naem A, Blackford SJI, Georgiadis A, Lakowski J, Hubank M, Smith AJ, Bainbridge JWB, Sowden JC, Ali RR (2013) Photoreceptor precursors derived from three-dimensional embryonic stem cell cultures integrate and mature within adult degenerate retina. *Nat Biotechnol* 31:741–747. <https://doi.org/10.1038/nbt.2643>
 44. Mears AJ, Kondo M, Swain PK, Takada Y, Bush RA, Saunders TL, Sieving PA, Swaroop A (2001) Nrl is required for rod photoreceptor development. *Nat Genet* 29:447–452. <https://doi.org/10.1038/ng774>
 45. Kruczek K, Gonzalez-Cordero A, Goh D, Naem A, Jonikas M, Blackford SJI, Kloc M, Duran Y, Georgiadis A, Sampson RD, Maswood RN, Smith AJ, Decembrini S, Arsenijevic Y, Sowden JC, Pearson RA, West EL, Ali RR (2017) Differentiation and transplantation of embryonic stem cell-derived cone photoreceptors into a mouse model of end-stage retinal degeneration. *Stem Cell Rep* 8:1659–1674. <https://doi.org/10.1016/j.stemcr.2017.04.030>
 46. Zhou PY, Peng GH, Xu H, Yin ZQ (2015) c-Kit+ cells isolated from human fetal retinas represent a new population of retinal progenitor cells. *J Cell Sci* 128:2169–2178. <https://doi.org/10.1242/jcs.169086>
 47. Zou T, Gao L, Zeng Y, Li Q, Li Y, Chen S, Hu X, Chen X, Fu C, Xu H, Yin ZQ (2019) Organoid-derived C-Kit(+)/SSEA4(-) human retinal progenitor cells promote a protective retinal micro-environment during transplantation in rodents. *Nat Commun* 10:1205. <https://doi.org/10.1038/s41467-019-08961-0>
 48. Lakowski J, Han YT, Pearson RA, Gonzalez-Cordero A, West EL, Gualdoni S, Barber AC, Hubank M, Ali RR, Sowden JC (2011) Effective transplantation of photoreceptor precursor cells selected via cell surface antigen expression. *Stem Cells* 29:1391–1404. <https://doi.org/10.1002/stem.694>
 49. Lakowski J, Gonzalez-Cordero A, West EL, Han YT, Welby E, Naem A, Blackford SJ, Bainbridge JW, Pearson RA, Ali RR, Sowden JC (2015) Transplantation of photoreceptor precursors isolated via a cell surface biomarker panel from embryonic stem cell-derived self-forming retina. *Stem Cells* 33:2469–2482. <https://doi.org/10.1002/stem.2051>
 50. Gagliardi G, Ben M'Barek K, Chaffiol A, Slembrouck-Brec A, Conart JB, Nanteau C, Rabesandratana O, Sahel JA, Duebel J, Orioux G, Reichman S, Goureau O (2018) Characterization and transplantation of CD73-positive photoreceptors isolated from human iPSC-derived retinal organoids. *Stem Cell Rep* 11:665–680. <https://doi.org/10.1016/j.stemcr.2018.07.005>
 51. Lakowski J, Welby E, Budinger D, Di Marco F, Di Foggia V, Bainbridge JWB, Wallace K, Gamm DM, Ali RR, Sowden JC (2018) Isolation of human photoreceptor precursors via a cell surface marker panel from stem cell-derived retinal organoids and fetal retinae. *STEM CELLS* 36:709–722. <https://doi.org/10.1002/stem.2775>
 52. Stone NE, Voigt AP, Cooke JA, Giacalone JC, Hanasoge S, Mullins RF, Tucker BA, Sulchek T (2020) Label-free microfluidic enrichment of photoreceptor cells. *Exp Eye Res* 199:108166. <https://doi.org/10.1016/j.exer.2020.108166>
 53. Santos-Ferreira TF, Borsch O, Ader M (2016) Rebuilding the missing part—a review on photoreceptor transplantation. *Front Syst Neurosci* 10:105. <https://doi.org/10.3389/fnsys.2016.00105>
 54. Schwartz SD, Regillo CD, Lam BL, Elliott D, Rosenfeld PJ, Gregori NZ, Hubschman JP, Davis JL, Heilwell G, Spirn M, Maguire J, Gay R, Bateman J, Ostrick RM, Morris D, Vincent M, Anglade E, Del Priore LV, Lanza R (2015) Human embryonic stem cell-derived retinal pigment epithelium in patients with age-related macular degeneration and Stargardt's macular dystrophy: follow-up of two open-label phase 1/2 studies. *Lancet* 385:509–516. [https://doi.org/10.1016/s0140-6736\(14\)61376-3](https://doi.org/10.1016/s0140-6736(14)61376-3)
 55. Singh MS, Park SS, Albini TA, Canto-Soler MV, Klassen H, MacLaren RE, Takahashi M, Nagiel A, Schwartz SD, Bharti K (2020) Retinal stem cell transplantation: balancing safety and potential. *Prog Retin Eye Res* 75:100779. <https://doi.org/10.1016/j.preteyeres.2019.100779>
 56. Assawachananont J, Mandai M, Okamoto S, Yamada C, Eiraku M, Yonemura S, Sasai Y, Takahashi M (2014) Transplantation of embryonic and induced pluripotent stem cell-derived 3D retinal sheets into retinal degenerative mice. *Stem Cell Reports* 2:662–674. <https://doi.org/10.1016/j.stemcr.2014.03.011>
 57. Shirai H, Mandai M, Matsushita K, Kuwahara A, Yonemura S, Nakano T, Assawachananont J, Kimura T, Saito K, Terasaki H, Eiraku M, Sasai Y, Takahashi M (2016) Transplantation of human embryonic stem cell-derived retinal tissue in two primate models of retinal degeneration. *Proc Natl Acad Sci U S A* 113:E81–90. <https://doi.org/10.1073/pnas.1512590113>
 58. Mandai M, Fujii M, Hashiguchi T, Sunagawa GA, Ito SI, Sun J, Kaneko J, Sho J, Yamada C, Takahashi M (2017) iPSC-derived retina transplants improve vision in rd1 end-stage retinal-degeneration mice. *Stem Cell Rep* 8:69–83. <https://doi.org/10.1016/j.stemcr.2016.12.008>
 59. McLelland BT, Lin B, Mathur A, Aramant RB, Thomas BB, Nistor G, Keirstead HS, Seiler MJ (2018) Transplanted hESC-derived retina organoid sheets differentiate, integrate, and improve visual function in retinal degenerate rats. *Invest Ophthalmol Vis Sci* 59:2586–2603. <https://doi.org/10.1167/iovs.17-23646>
 60. Singh RK, Occelli LM, Binette F, Petersen-Jones SM, Nasonkin IO (2019) Transplantation of human embryonic stem cell-derived retinal tissue in the subretinal space of the cat eye. *Stem Cells Dev* 28:1151–1166. <https://doi.org/10.1089/scd.2019.0090>
 61. Tu HY, Watanabe T, Shirai H, Yamasaki S, Kinoshita M, Matsushita K, Hashiguchi T, Onoe H, Matsuyama T, Kuwahara A, Kishino A, Kimura T, Eiraku M, Suzuma K, Kitaoka T, Takahashi M, Mandai M (2019) Medium- to long-term survival and functional examination of human iPSC-derived retinas in rat and

- primate models of retinal degeneration. *EBioMedicine* 39:562–574. <https://doi.org/10.1016/j.ebiom.2018.11.028>
62. West EL, Pearson RA, Tschernutter M, Sowden JC, MacLaren RE, Ali RR (2008) Pharmacological disruption of the outer limiting membrane leads to increased retinal integration of transplanted photoreceptor precursors. *Exp Eye Res* 86:601–611. <https://doi.org/10.1016/j.exer.2008.01.004>
 63. Pearson RA, Barber AC, West EL, MacLaren RE, Duran Y, Bainbridge JW, Sowden JC, Ali RR (2010) Targeted disruption of outer limiting membrane junctional proteins (Crb1 and ZO-1) increases integration of transplanted photoreceptor precursors into the adult wild-type and degenerating retina. *Cell Transplant* 19:487–503. <https://doi.org/10.3727/096368909x486057>
 64. Barber AC, Hippert C, Duran Y, West EL, Bainbridge JW, Warre-Cornish K, Luhmann UF, Lakowski J, Sowden JC, Ali RR, Pearson RA (2013) Repair of the degenerate retina by photoreceptor transplantation. *Proc Natl Acad Sci U S A* 110:354–359. <https://doi.org/10.1073/pnas.1212677110>
 65. Srivastava A (2016) In vivo tissue-tropism of adeno-associated viral vectors. *Curr Opin Virol* 21:75–80. <https://doi.org/10.1016/j.coviro.2016.08.003>
 66. Auricchio A, Kobinger G, Anand V, Hildinger M, O'Connor E, Maguire AM, Wilson JM, Bennett J (2001) Exchange of surface proteins impacts on viral vector cellular specificity and transduction characteristics: the retina as a model. *Hum Mol Genet* 10:3075–3081. <https://doi.org/10.1093/hmg/10.26.3075>
 67. Klimczak RR, Koerber JT, Dalkara D, Flannery JG, Schaffer DV (2009) A novel adeno-associated viral variant for efficient and selective intravitreal transduction of rat Müller cells. *PLoS ONE* 4:e7467. <https://doi.org/10.1371/journal.pone.0007467>
 68. Gonzalez-Cordero A, Goh D, Kruczek K, Naeem A, Fernando M, Kleine Holthaus SM, Takaaki M, Blackford SJI, Kloc M, Agundez L, Sampson RD, Borooah S, Ovando-Roche P, Mehat MS, West EL, Smith AJ, Pearson RA, Ali RR (2018) Assessment of AAV vector tropisms for mouse and human pluripotent stem cell-derived RPE and photoreceptor cells. *Hum Gene Ther* 29:1124–1139. <https://doi.org/10.1089/hum.2018.027>
 69. Khabou H, Garita-Hernandez M, Chaffiol A, Reichman S, Jaillard C, Brazhnikova E, Bertin S, Forster V, Desrosiers M, Winckler C, Goureau O, Picaud S, Duebel J, Sahel J-A, Dalkara D (2018) Noninvasive gene delivery to foveal cones for vision restoration. *JCI Insight*. <https://doi.org/10.1172/jci.insight.96029>
 70. Garita-Hernandez M, Routet F, Guibbal L, Khabou H, Toulbi L, Riancho L, Reichman S, Duebel J, Sahel J-A, Goureau O, Dalkara D (2020) AAV-mediated gene delivery to 3D retinal organoids derived from human induced pluripotent stem cells. *Int J Mol Sci* 21:99. <https://doi.org/10.3390/ijms21030994>
 71. Lane A, Jovanovic K, Shortall C, Ottaviani D, Panes AB, Schwarz N, Guarascio R, Hayes MJ, Palfi A, Chadderton N, Farrar GJ, Hardcastle AJ, Cheetham ME (2020) Modelling and rescue of RP2 retinitis pigmentosa using iPSC derived retinal organoids. *Stem Cell Rep* 15:67–79. <https://doi.org/10.1016/j.stemcr.2020.05.007>
 72. Achberger K, Cipriano M, Düchs M, Schön C, Michelfelder S, Stierstorfer B, Lamla T, Kauschke SG, Chuchuy J, Roosz J, Mesch L, Cora V, Pars S, Pashkovskaia N, Corti S, Kleger A, Kreuz S, Maier U, Liebau S, Loskill P (2021) Human stem cell-based retina-on-chip as new translational model for validation of AAV retinal gene therapy vectors. *bioRxiv*. <https://doi.org/10.1101/2021.03.02.433550>
 73. Pavlou M, Schön C, Occelli LM, Rossi A, Meumann N, Boyd RF, Bartoe JT, Siedlecki J, Gerhardt MJ, Babutzka S, Bogedain J, Wagner JE, Priglinger SG, Biel M, Petersen-Jones SM, Büning H, Michalakis S (2021) Novel AAV capsids for intravitreal gene therapy of photoreceptor disorders. *EMBO Mol Med*. <https://doi.org/10.15252/emmm.202013392>
 74. Völkner M, Pavlou M, Büning H, Michalakis S, Karl M (2021) Optimized adeno-associated virus vectors for efficient transduction of human retinal organoids. *Hum Gene Ther*. <https://doi.org/10.1089/hum.2020.321>
 75. Madrakhimov SB, Yang JY, Ahn DH, Han JW, Ha TH, Park TK (2020) Peripapillary intravitreal injection improves AAV-mediated retinal transduction. *Mol Ther Methods Clin Dev* 17:647–656. <https://doi.org/10.1016/j.omtm.2020.03.018>
 76. Vázquez-Domínguez I, Garanto A, Collin RWJ (2019) Molecular therapies for inherited retinal diseases-current standing, opportunities and challenges. *Genes* 10:654. <https://doi.org/10.3390/genes10090654>
 77. Collin RW, Garanto A (2017) Applications of antisense oligonucleotides for the treatment of inherited retinal diseases. *Curr Opin Ophthalmol* 28:260–266. <https://doi.org/10.1097/icu.0000000000000363>
 78. Parfitt DA, Lane A, Ramsden CM, Carr AJ, Munro PM, Jovanovic K, Schwarz N, Kanuga N, Muthiah MN, Hull S, Gallo JM, da Cruz L, Moore AT, Hardcastle AJ, Coffey PJ, Cheetham ME (2016) Identification and correction of mechanisms underlying inherited blindness in human iPSC-derived optic cups. *Cell Stem Cell* 18:769–781. <https://doi.org/10.1016/j.stem.2016.03.021>
 79. Dulla K, Aguila M, Lane A, Jovanovic K, Parfitt DA, Schulzens I, Chan HL, Schmidt I, Beumer W, Vorthoren L, Collin RWJ, Garanto A, Duijkers L, Brugulat-Panes A, Semo M, Vugler AA, Biasutto P, Adamson P, Cheetham ME (2018) Splice-modulating oligonucleotide QR-110 restores CEP290 mRNA and function in human c.2991+1655A>G LCA10 models. *Mol Ther Nucleic Acids* 12:730–740. <https://doi.org/10.1016/j.omtn.2018.07.010>
 80. Khan M, Arno G, Fakin A, Parfitt DA, Dhooze PPA, Albert S, Bax NM, Duijkers L, Niblock M, Hau KL, Bloch E, Schiff ER, Piccolo D, Hogden MC, Hoyng CB, Webster AR, Cremers FPM, Cheetham ME, Garanto A, Collin RWJ (2020) Detailed phenotyping and therapeutic strategies for intronic ABCA4 variants in stargardt disease. *Mol Ther Nucleic Acids* 21:412–427. <https://doi.org/10.1016/j.omtn.2020.06.007>
 81. Dulla K, Slijkerman R, van Diepen HC, Albert S, Dona M, Beumer W, Turunen JJ, Chan HL, Schulzens IA, Vorthoren L, den Besten C, Buil L, Schmidt I, Miao J, Venselaar H, Zang J, Neuhaus SCF, Peters T, Broekman S, Pennings R, Kremer H, Platenburg G, Adamson P, de Vrieze E, van Wijk E (2021) Antisense oligonucleotide-based treatment of retinitis pigmentosa caused by USH2A exon 13 mutations. *Mol Ther*. <https://doi.org/10.1016/j.yjmt.2021.04.024>
 82. Díaz N, Kruse K, Erdmann T, Staiger AM, Ott G, Lenz G, Vaquerizas JM (2018) Chromatin conformation analysis of primary patient tissue using a low input Hi-C method. *Nat Commun* 9:4938. <https://doi.org/10.1038/s41467-018-06961-0>
 83. Rao Suhas SP, Huntley Miriam H, Durand Neva C, Stamenov Elena K, Bochkov Ivan D, Robinson James T, Sanborn Adrian L, Machol I, Omer Arina D, Lander Eric S, Aiden Erez L (2014) A 3D map of the human genome at kilobase resolution reveals principles of chromatin looping. *Cell* 159:1665–1680. <https://doi.org/10.1016/j.cell.2014.11.021>
 84. de Bruijn SE, Fiorentino A, Ottaviani D, Fanucchi S, Melo US, Corral-Serrano JC, Mulders T, Georgiou M, Rivolta C, Pontikos N, Arno G, Roberts L, Greenberg J, Albert S, Gilissen C, Aben M, Rebello G, Mead S, Raymond FL, Corominas J, Smith CEL, Kremer H, Downes S, Black GC, Webster AR, Inglehearn CF, van den Born LI, Koenekoop RK, Michaelides M, Ramesar RS, Hoyng CB, Mundlos S, Mhlanga MM, Cremers FPM, Cheetham ME, Roosing S, Hardcastle AJ (2020) Structural variants create new topological-associated domains and ectopic retinal enhancer-gene contact in dominant retinitis

- pigmentosa. *Am J Human Genetics* 107:802–814. <https://doi.org/10.1016/j.ajhg.2020.09.002>
85. Buenrostro JD, Giresi PG, Zaba LC, Chang HY, Greenleaf WJ (2013) Transposition of native chromatin for fast and sensitive epigenomic profiling of open chromatin, DNA-binding proteins and nucleosome position. *Nat Methods* 10:1213–1218. <https://doi.org/10.1038/nmeth.2688>
 86. Wang J, Zibetti C, Shang P, Sripathi SR, Zhang P, Cano M, Hoang T, Xia S, Ji H, Merbs SL, Zack DJ, Handa JT, Sinha D, Blackshaw S, Qian J (2018) ATAC-Seq analysis reveals a widespread decrease of chromatin accessibility in age-related macular degeneration. *Nat Commun* 9:1364–1364. <https://doi.org/10.1038/s41467-018-03856-y>
 87. Jager RD, Mieler WF, Miller JW (2008) Age-related macular degeneration. *N Engl J Med* 358:2606–2617. <https://doi.org/10.1056/NEJMra0801537>
 88. Saiki R, Scharf S, Faloona F, Mullis K, Horn G, Erlich H, Arnheim N (1985) Enzymatic amplification of beta-globin genomic sequences and restriction site analysis for diagnosis of sickle cell anemia. *Science* 230:1350–1354. <https://doi.org/10.1126/science.2999980>
 89. Freeman WM, Walker SJ, Vrana KE (1999) Quantitative RT-PCR: pitfalls and potential. *Biotechniques* 26:112–125. <https://doi.org/10.2144/99261rv01>
 90. Xu W, Seok J, Mindrinos MN, Schweitzer AC, Jiang H, Wilhelmly J, Clark TA, Kapur K, Xing Y, Faham M, Storey JD, Moldawer LL, Maier RV, Tompkins RG, Wong WH, Davis RW, Xiao W (2011) Human transcriptome array for high-throughput clinical studies. *Proc Natl Acad Sci U S A* 108:3707–3712. <https://doi.org/10.1073/pnas.1019753108>
 91. Binder H, Preibisch S (2005) Specific and nonspecific hybridization of oligonucleotide probes on microarrays. *Biophys J* 89:337–352. <https://doi.org/10.1529/biophysj.104.055343>
 92. Kaewkhaw R, Kaya KD, Brooks M, Homma K, Zou J, Chaitankar V, Rao M, Swaroop A (2015) Transcriptome dynamics of developing photoreceptors in three-dimensional retina cultures recapitulates temporal sequence of human cone and rod differentiation revealing cell surface markers and gene networks. *Stem Cells* 33:3504–3518. <https://doi.org/10.1002/stem.2122>
 93. Welby E, Lakowski J, Di Foggia V, Budinger D, Gonzalez-Cordero A, Lun ATL, Epstein M, Patel A, Cuevas E, Kruczek K, Naem A, Minneci F, Hubank M, Jones DT, Marioni JC, Ali RR, Sowden JC (2017) Isolation and comparative transcriptome analysis of human fetal and iPSC-derived cone photoreceptor cells. *Stem Cell Rep* 9:1898–1915. <https://doi.org/10.1016/j.stemcr.2017.10.018>
 94. Chu L-F, Leng N, Zhang J, Hou Z, Mamott D, Vereide DT, Choi J, Kendzioriski C, Stewart R, Thomson JA (2016) Single-cell RNA-seq reveals novel regulators of human embryonic stem cell differentiation to definitive endoderm. *Genome Biol* 17:173. <https://doi.org/10.1186/s13059-016-1033-x>
 95. Phillips MJ, Jiang P, Howden S, Barney P, Min J, York NW, Chu LF, Capowski EE, Cash A, Jain S, Barlow K, Tabassum T, Stewart R, Pattnaik BR, Thomson JA, Gamm DM (2018) A novel approach to single cell RNA-sequence analysis facilitates in silico gene reporting of human pluripotent stem cell-derived retinal cell types. *Stem Cells* 36:313–324. <https://doi.org/10.1002/stem.2755>
 96. Collin J, Queen R, Zerti D, Dorgau B, Hussain R, Coxhead J, Cockell S, Lako M (2019) Deconstructing retinal organoids: single cell RNA-Seq reveals the cellular components of human pluripotent stem cell-derived retina. *Stem Cells* 37:593–598. <https://doi.org/10.1002/stem.2963>
 97. Kim S, Lowe A, Dharmat R, Lee S, Owen LA, Wang J, Shakoor A, Li Y, Morgan DJ, Hejazi AA, Cvekl A, DeAngelis MM, Zhou ZJ, Chen R, Liu W (2019) Generation, transcriptome profiling, and functional validation of cone-rich human retinal organoids. *Proc Natl Acad Sci U S A* 116:10824–10833. <https://doi.org/10.1073/pnas.1901572116>
 98. Lu Y, Shiao F, Yi W, Lu S, Wu Q, Pearson JD, Kallman A, Zhong S, Hoang T, Zuo Z, Zhao F, Zhang M, Tsai N, Zhuo Y, He S, Zhang J, Stein-O'Brien GL, Sherman TD, Duan X, Fertig EJ, Goff LA, Zack DJ, Handa JT, Xue T, Bremner R, Blackshaw S, Wang X, Clark BS (2020) Single-cell analysis of human retina identifies evolutionarily conserved and species-specific mechanisms controlling development. *Dev Cell* 53:473–491.e9. <https://doi.org/10.1016/j.devcel.2020.04.009>
 99. Pasquini G, Cora V, Swiersy A, Achberger K, Antkowiak L, Müller B, Wimmer T, Fraschka SA, Casadei N, Ueffing M, Liebau S, Stieger K, Buskamp V (2020) Using transcriptomic analysis to assess double-strand break repair activity: towards precise in vivo genome editing. *Int J Mol Sci* 21:1380. <https://doi.org/10.3390/ijms21041380>
 100. Buskin A, Zhu L, Chichagova V, Basu B, Mozaffari-Jovin S, Dolan D, Droop A, Collin J, Bronstein R, Mehrotra S, Farkas M, Hilgen G, White K, Pan K-T, Treumann A, Hallam D, Bialas K, Chung G, Mellough C, Ding Y, Krasnogor N, Przyborski S, Zwolinski S, Al-Aama J, Alharthi S, Xu Y, Wheway G, Szymanska K, McKibbin M, Inglehearn CF, Elliott DJ, Lindsay S, Ali RR, Steel DH, Armstrong L, Sernagor E, Urlaub H, Pierce E, Lührmann R, Grellscheid S-N, Johnson CA, Lako M (2018) Disrupted alternative splicing for genes implicated in splicing and ciliogenesis causes PRPF31 retinitis pigmentosa. *Nat Commun* 9:4234–4234. <https://doi.org/10.1038/s41467-018-06448-y>
 101. Lukovic D, Artero Castro A, Kaya KD, Munezero D, Gieser L, Davo-Martinez C, Corton M, Cuenca N, Swaroop A, Ramamurthy V, Ayuso C, Erceg S (2020) Retinal organoids derived from hiPSCs of an AIPL1-LCA patient maintain cytoarchitecture despite reduced levels of mutant AIPL1. *Sci Rep* 10:5426. <https://doi.org/10.1038/s41598-020-62047-2>
 102. Deng W-L, Gao M-L, Lei X-L, Lv J-N, Zhao H, He K-W, Xia X-X, Li L-Y, Chen Y-C, Li Y-P, Pan D, Xue T, Jin Z-B (2018) Gene correction reverses ciliopathy and photoreceptor loss in iPSC-derived retinal organoids from retinitis pigmentosa patients. *Stem Cell Rep* 10:1267–1281. <https://doi.org/10.1016/j.stemcr.2018.02.003>
 103. Huang KC, Wang ML, Chen SJ, Kuo JC, Wang WJ, Nhi Nguyen PN, Wahlin KJ, Lu JF, Tran AA, Shi M, Chien Y, Yarmishyn AA, Tsai PH, Yang TC, Jane WN, Chang CC, Peng CH, Schlaeger TM, Chiou SH (2019) Morphological and molecular defects in human three-dimensional retinal organoid model of X-linked Juvenile Retinoschisis. *Stem Cell Rep* 13:906–923. <https://doi.org/10.1016/j.stemcr.2019.09.010>
 104. Sundar J, Matalkah F, Jeong B, Stoilov P, Ramamurthy V (2020) The Musashi proteins MSI1 and MSI2 are required for photoreceptor morphogenesis and vision in mice. *J Biol Chem* 296:100048. <https://doi.org/10.1074/jbc.RA120.015714>
 105. Ling JP, Wilks C, Charles R, Leavey PJ, Ghosh D, Jiang L, Santiago CP, Pang B, Venkataraman A, Clark BS, Nellore A, Langmead B, Blackshaw S (2020) ASCOT identifies key regulators of neuronal subtype-specific splicing. *Nat Commun* 11:137. <https://doi.org/10.1038/s41467-019-14020-5>
 106. Cideciyan AV, Jacobson SG, Drack AV, Ho AC, Charng J, Garafalo AV, Roman AJ, Sumaroka A, Han IC, Hochstedler MD, Pfeifer WL, Sohn EH, Taiel M, Schwartz MR, Biasutto P, Wit W, Cheetham ME, Adamson P, Rodman DM, Platenburg G, Tome MD, Balikova I, Nerinckx F, Zaeytjij D, Van Cauwenbergh C, Leroy BP, Russell SR (2019) Effect of an intravitreal antisense oligonucleotide on vision in Leber congenital amaurosis due to a photoreceptor cilium defect. *Nat Med* 25:225–228. <https://doi.org/10.1038/s41591-018-0295-0>

107. Arno G, Agrawal SA, Eblimit A, Bellingham J, Xu M, Wang F, Chakarova C, Parfitt DA, Lane A, Burgoyne T, Hull S, Carss KJ, Fiorentino A, Hayes MJ, Munro PM, Nicols R, Pontikos N, Holder GE, Ukirdc AC, Raymond FL, Moore AT, Plagnol V, Michaelides M, Hardcastle AJ, Li Y, Cukras C, Webster AR, Cheetham ME, Chen R (2016) Mutations in REEP6 cause autosomal-recessive retinitis pigmentosa. *Am J Hum Genet* 99:1305–1315. <https://doi.org/10.1016/j.ajhg.2016.10.008>
108. Vig A, Poulter JA, Ottaviani D, Tavares E, Toropova K, Traceswska AM, Mollica A, Kang J, Kehelwathugoda O, Paton T, Maynes JT, Wheway G, Arno G, Khan KN, McKibbin M, Toomes C, Ali M, Di Scipio M, Li S, Ellingford J, Black G, Webster A, Rydzanicz M, Stawiński P, Płoski R, Vincent A, Cheetham ME, Inglehearn CF, Roberts A, Heon E (2020) DYNC2H1 hypomorphic or retina-predominant variants cause nonsyndromic retinal degeneration. *Genet Med* 22:2041–2051. <https://doi.org/10.1038/s41436-020-0915-1>
109. Conesa A, Madrigal P, Tarazona S, Gomez-Cabrero D, Cervera A, McPherson A, Szczeniak MW, Gaffney DJ, Elo LL, Zhang X, Mortazavi A (2016) A survey of best practices for RNA-seq data analysis. *Genome Biol* 17:13. <https://doi.org/10.1186/s13059-016-0881-8>
110. Tilgner H, Jahanbani F, Blauwkamp T, Moshrefi A, Jaeger E, Chen F, Harel I, Bustamante CD, Rasmussen M, Snyder MP (2015) Comprehensive transcriptome analysis using synthetic long-read sequencing reveals molecular co-association of distant splicing events. *Nat Biotechnol* 33:736–742. <https://doi.org/10.1038/nbt.3242>
111. Ghazalpour A, Bennett B, Petyuk VA, Orozco L, Hagopian R, Mungrue IN, Farber CR, Sinsheimer J, Kang HM, Furlotte N, Park CC, Wen PZ, Brewer H, Weitz K, Camp DG 2nd, Pan C, Yordanova R, Neuhaus I, Tilford C, Siemers N, Gargalovic P, Eskin E, Kirchgessner T, Smith DJ, Smith RD, Lusk AJ (2011) Comparative analysis of proteome and transcriptome variation in mouse. *PLoS Genet* 7:e1001393. <https://doi.org/10.1371/journal.pgen.1001393>
112. Yeung ES (2011) Genome-wide correlation between mRNA and protein in a single cell. *Angew Chem Int Ed Engl* 50:583–585. <https://doi.org/10.1002/anie.201005969>
113. Towbin H, Staehelin T, Gordon J (1979) Electrophoretic transfer of proteins from polyacrylamide gels to nitrocellulose sheets: procedure and some applications. *Proc Natl Acad Sci U S A* 76:4350–4354. <https://doi.org/10.1073/pnas.76.9.4350>
114. Sharma TP, Wiley LA, Whitmore SS, Anfinson KR, Cranston CM, Oppedal DJ, Daggett HT, Mullins RF, Tucker BA, Stone EM (2017) Patient-specific induced pluripotent stem cells to evaluate the pathophysiology of TRNT1-associated Retinitis pigmentosa. *Stem Cell Res* 21:58–70. <https://doi.org/10.1016/j.scr.2017.03.005>
115. Phillips MJ, Perez ET, Martin JM, Reshel ST, Wallace KA, Capowski EE, Singh R, Wright LS, Clark EM, Barney PM, Stewart R, Dickerson SJ, Miller MJ, Percin EF, Thomson JA, Gamm DM (2014) Modeling human retinal development with patient-specific induced pluripotent stem cells reveals multiple roles for visual system homeobox 2. *Stem Cells* 32:1480–1492. <https://doi.org/10.1002/stem.1667>
116. Peskova L, Jurcikova D, Vanova T, Krivanek J, Capandova M, Sramkova Z, Kolouskova M, Kotasova H, Streit L, Barta T (2020) miR-183/96/182 cluster is an important morphogenetic factor targeting PAX6 expression in differentiating human retinal organoids. *Stem Cells* 38:1557–1567. <https://doi.org/10.1002/stem.3272>
117. Boellner S, Becker K-F (2015) Reverse phase protein arrays-quantitative assessment of multiple biomarkers in biopsies for clinical use. *Microarrays* 4:98–114. <https://doi.org/10.3390/microarrays4020098>
118. Wiese S, Reidegeld KA, Meyer HE, Warscheid B (2007) Protein labeling by iTRAQ: a new tool for quantitative mass spectrometry in proteome research. *Proteomics* 7:340–350. <https://doi.org/10.1002/pmic.200600422>
119. Ong SE, Blagoev B, Kratchmarova I, Kristensen DB, Steen H, Pandey A, Mann M (2002) Stable isotope labeling by amino acids in cell culture, SILAC, as a simple and accurate approach to expression proteomics. *Mol Cell Proteomics* 1:376–386. <https://doi.org/10.1074/mcp.m200025-mcp200>
120. Clish CB (2015) Metabolomics: an emerging but powerful tool for precision medicine. *Cold Spring Harb Mol Case Stud* 1:a000588. <https://doi.org/10.1101/mcs.a000588>
121. Tan SZ, Begley P, Mullard G, Hollywood KA, Bishop PN (2016) Introduction to metabolomics and its applications in ophthalmology. *Eye* 30:773–783. <https://doi.org/10.1038/eye.2016.37>
122. Laíns I, Gantner M, Murinello S, Lasky-Su JA, Miller JW, Friedlander M, Husain D (2019) Metabolomics in the study of retinal health and disease. *Prog Retin Eye Res* 69:57–79. <https://doi.org/10.1016/j.preteyeres.2018.11.002>
123. Weygand J, Carter S, Salzillo T, Moussalli M, Dai B, Dutta P, Zuo X, Fleming J, Shureiqi I, Bhattacharya P (2017) Can an organoid recapitulate the metabolome of its parent tissue? A pilot NMR spectroscopy study. *J Cancer Prev Curr Res*. <https://doi.org/10.15406/jcpcr.2017.08.00307>
124. Aqeilan RI (2021) Engineering organoids: a promising platform to understand biology and treat diseases. *Cell Death Differ* 28:1–4. <https://doi.org/10.1038/s41418-020-00680-0>
125. Lindeboom RG, van Voorthuisen L, Oost KC, Rodríguez-Colman MJ, Luna-Velez MV, Furlan C, Baraille F, Jansen PW, Ribeiro A, Burgering BM, Snippert HJ, Vermeulen M (2018) Integrative multi-omics analysis of intestinal organoid differentiation. *Mol Syst Biol* 14:e8227. <https://doi.org/10.15252/msb.20188227>
126. Okkelman IA, Neto N, Papkovsky DB, Monaghan MG, Dmitriev RI (2020) A deeper understanding of intestinal organoid metabolism revealed by combining fluorescence lifetime imaging microscopy (FLIM) and extracellular flux analyses. *Redox Biol* 30:101420. <https://doi.org/10.1016/j.redox.2019.101420>
127. Browne AW, Arnesano C, Harutyunyan N, Khuu T, Martinez JC, Pollack HA, Koos DS, Lee TC, Fraser SE, Moats RA, Aparicio JG, Cobrinik D (2017) Structural and functional characterization of human stem-cell-derived retinal organoids by live imaging. *Invest Ophthalmol Vis Sci* 58:3311–3318. <https://doi.org/10.1167/iovs.16-20796>
128. Scholler J, Groux K, Goureau O, Sahel J-A, Fink M, Reichman S, Boccara C, Grieve K (2020) Dynamic full-field optical coherence tomography: 3D live-imaging of retinal organoids. *Light, Sci Appl* 9:140–140. <https://doi.org/10.1038/s41377-020-00375-8>
129. Hallam D, Hilgen G, Dorgau B, Zhu L, Yu M, Bojic S, Hewitt P, Schmitt M, Uteng M, Kustermann S, Steel D, Nicholds M, Thomas R, Treumann A, Porter A, Sernagor E, Armstrong L, Lako M (2018) Human-induced pluripotent stem cells generate light responsive retinal organoids with variable and nutrient-dependent efficiency. *Stem Cells* 36:1535–1551. <https://doi.org/10.1002/stem.2883>
130. Willems E, Lorés-Motta L, Zanichelli A, Suffritti C, van der Flier M, van der Molen RG, Langereis JD, van Drongelen J, van den Heuvel LP, Volokhina E, van de Kar NC, Keizer-Garritsen J, Levin M, Herberg JA, Martinon-Torres F, Wessels HJ, de Breuk A, Fauser S, Hoyng CB, den Hollander AI, de Groot R, van Gool AJ, Gloerich J, de Jonge MI (2020) Quantitative multiplex profiling of the complement system to diagnose complement-mediated diseases. *Clin Transl Immunol* 9:e1225. <https://doi.org/10.1002/cti2.1225>

131. Hancock RJ, Yendle JE, Bradley BA (1989) MicroELISA assays of anti-HLA activity and isotype of human monoclonal antibodies. *Tissue Antigens* 33:437–444. <https://doi.org/10.1111/j.1399-0039.1989.tb01692.x>
132. Kremlitzka M, Geerlings MJ, de Jong S, Bakker B, Nilsson SC, Fauser S, Hoyng CB, de Jong EK, den Hollander AI, Blom AM (2018) Functional analyses of rare genetic variants in complement component C9 identified in patients with age-related macular degeneration. *Hum Mol Genet* 27:2678–2688. <https://doi.org/10.1093/hmg/ddy178>
133. de Jong S, Volokhina EB, de Breuk A, Nilsson SC, de Jong EK, van der Kar N, Bakker B, Hoyng CB, van den Heuvel LP, Blom AM, den Hollander AI (2020) Effect of rare coding variants in the CFI gene on Factor I expression levels. *Hum Mol Genet* 29:2313–2324. <https://doi.org/10.1093/hmg/ddaa114>
134. Stiles M, Qi H, Sun E, Tan J, Porter H, Allegood J, Chalfant CE, Yasumura D, Matthes MT, LaVail MM, Mandal NA (2016) Sphingolipid profile alters in retinal dystrophic P23H–I rats and systemic FTY720 can delay retinal degeneration. *J Lipid Res* 57:818–831. <https://doi.org/10.1194/jlr.M063719>
135. Pereiro X, Fernández R, Barreda-Gómez G, Ruzafa N, Acera A, Araiz J, Astigarraga E, Vecino E (2020) Comparative lipidomic analysis of mammalian retinal ganglion cells and Müller glia in situ and in vitro using high-resolution imaging mass spectrometry. *Sci Rep* 10:20053. <https://doi.org/10.1038/s41598-020-77087-x>
136. Sibille E, Berdeaux O, Martine L, Bron AM, Creuzot-Garcher CP, He Z, Thuret G, Bretillon L, Masson EA (2016) Ganglioside profiling of the human retina: comparison with other ocular structures, brain and plasma reveals tissue specificities. *PLoS ONE* 11:e0168794. <https://doi.org/10.1371/journal.pone.0168794>
137. Zhuo C, Hou W, Tian H, Wang L, Li R (2020) Lipidomics of the brain, retina, and biofluids: from the biological landscape to potential clinical application in schizophrenia. *Transl Psychiatry* 10:391. <https://doi.org/10.1038/s41398-020-01080-1>
138. Brush RS, Tran JT, Henry KR, McClellan ME, Elliott MH, Mandal MN (2010) Retinal sphingolipids and their very-long-chain fatty acid-containing species. *Invest Ophthalmol Vis Sci* 51:4422–4431. <https://doi.org/10.1167/iovs.09-5134>
139. Acar N, Berdeaux O, Grégoire S, Cabaret S, Martine L, Gain P, Thuret G, Creuzot-Garcher CP, Bron AM, Bretillon L (2012) Lipid composition of the human eye: are red blood cells a good mirror of retinal and optic nerve fatty acids? *PLoS ONE* 7:e35102. <https://doi.org/10.1371/journal.pone.0035102>
140. Ford DA, Monda JK, Brush RS, Anderson RE, Richards MJ, Fliesler SJ (2008) Lipidomic analysis of the retina in a rat model of Smith-Lemli-Opitz syndrome: alterations in docosahexaenoic acid content of phospholipid molecular species. *J Neurochem* 105:1032–1047. <https://doi.org/10.1111/j.1471-4159.2007.05203.x>
141. Garanto A, Mandal NA, Egado-Gabás M, Marfany G, Fabriàs G, Anderson RE, Casas J, González-Duarte R (2013) Specific sphingolipid content decrease in Cerkl knockdown mouse retinas. *Exp Eye Res* 110:96–106. <https://doi.org/10.1016/j.exer.2013.03.003>
142. Gantner ML, Eade K, Wallace M, Handzlik MK, Fallon R, Trombley J, Bonelli R, Giles S, Harkins-Perry S, Heeren TFC, Sauer L, Ideguchi Y, Baldini M, Scheppeke L, Dorrell MI, Kitano M, Hart BJ, Cai C, Nagasaki T, Badur MG, Okada M, Woods SM, Egan C, Gillies M, Guymer R, Eichler F, Bahlo M, Fruttiger M, Allikmets R, Bernstein PS, Metallo CM, Friedlander M (2019) Serine and lipid metabolism in macular disease and peripheral neuropathy. *N Engl J Med* 381:1422–1433. <https://doi.org/10.1056/NEJMoa1815111>
143. Coons AH, Creech HJ, Norman JR, Berliner E (1942) The demonstration of pneumococcal antigen in tissues by the use of fluorescent antibody. *J Immunol* 45:159–170
144. Zheng C, Schneider JW, Hsieh J (2020) Role of RB1 in human embryonic stem cell-derived retinal organoids. *Dev Biol* 462:197–207. <https://doi.org/10.1016/j.ydbio.2020.03.011>
145. Svoboda K, Yasuda R (2006) Principles of two-photon excitation microscopy and its applications to neuroscience. *Neuron* 50:823–839. <https://doi.org/10.1016/j.neuron.2006.05.019>
146. Power RM, Huisken J (2017) A guide to light-sheet fluorescence microscopy for multiscale imaging. *Nat Methods* 14:360–373. <https://doi.org/10.1038/nmeth.4224>
147. Cora V, Haderspeck J, Antkowiak L, Mattheus U, Neckel PH, Mack AF, Bolz S, Ueffing M, Pashkovskaia N, Achberger K, Liebau S (2019) A cleared view on retinal organoids. *Cells*. <https://doi.org/10.3390/cells8050391>
148. Yang B, Treweek Jennifer B, Kulkarni Rajan P, Deverman Benjamin E, Chen C-K, Lubeck E, Shah S, Cai L, Gradinaru V (2014) Single-cell phenotyping within transparent intact tissue through whole-body clearing. *Cell* 158:945–958. <https://doi.org/10.1016/j.cell.2014.07.017>
149. Belle M, Godefroy D, Dominici C, Heitz-Marchaland C, Zelina P, Hellal F, Bradke F, Chédotal A (2014) A simple method for 3D analysis of immunolabeled axonal tracts in a transparent nervous system. *Cell Rep* 9:1191–1201. <https://doi.org/10.1016/j.celrep.2014.10.037>
150. Reichman S, Slembrouck A, Gagliardi G, Chaffiol A, Terray A, Nanteau C, Potey A, Belle M, Rabesandratana O, Duebel J, Orioux G, Nandrot EF, Sahel JA, Goureau O (2017) Generation of storable retinal organoids and retinal pigmented epithelium from adherent human iPSC cells in xeno-free and feeder-free conditions. *Stem Cells* 35:1176–1188. <https://doi.org/10.1002/stem.2586>
151. Vergara MN, Flores-Bellver M, Aparicio-Domingo S, McNally M, Wahlin KJ, Saxena MT, Mumm JS, Canto-Soler MV (2017) Three-dimensional automated reporter quantification (3D-ARQ) technology enables quantitative screening in retinal organoids. *Development* 144:3698–3705. <https://doi.org/10.1242/dev.146290>
152. Quinn PM, Buck TM, Mulder AA, Ohonin C, Alves CH, Vos RM, Bialecka M, van Herwaarden T, van Dijk EHC, Talib M, Freund C, Mikkers HMM, Hoeben RC, Goumans M-J, Boon CJF, Koster AJ, de Sousa C, Lopes SM, Jost CR, Wijnholds J (2019) Human iPSC-derived retinas recapitulate the fetal CRB1 CRB2 complex formation and demonstrate that photoreceptors and Müller glia are targets of AAV5. *Stem Cell Rep* 12:906–919. <https://doi.org/10.1016/j.stemcr.2019.03.002>
153. Ovando-Roche P, West EL, Branch MJ, Sampson RD, Fernando M, Munro P, Georgiadis A, Rizzi M, Kloc M, Naeem A, Ribeiro J, Smith AJ, Gonzalez-Cordero A, Ali RR (2018) Use of bioreactors for culturing human retinal organoids improves photoreceptor yields. *Stem Cell Res Ther* 9:156. <https://doi.org/10.1186/s13287-018-0907-0>
154. Burgoyne T, Lane A, Laughlin WE, Cheetham ME, Futter CE (2018) Correlative light and immuno-electron microscopy of retinal tissue cryostat sections. *PLoS ONE* 13:e0191048. <https://doi.org/10.1371/journal.pone.0191048>
155. Kornreich BG (2007) The patch clamp technique: principles and technical considerations. *J Vet Cardiol* 9:25–37. <https://doi.org/10.1016/j.jvc.2007.02.001>
156. Neher E, Sakmann B (1976) Single-channel currents recorded from membrane of denervated frog muscle fibres. *Nature* 260:799–802. <https://doi.org/10.1038/260799a0>
157. Hurley JB (2009) Phototransduction. In: Squire LR (ed) *Encyclopedia of neuroscience*. Academic Press, Oxford, pp 687–692

158. Sandell JH (1998) GABA as a developmental signal in the inner retina and optic nerve. *Perspect Dev Neurobiol* 5:269–278
159. Meyer JS, Howden SE, Wallace KA, Verhoeven AD, Wright LS, Capowski EE, Pinilla I, Martin JM, Tian S, Stewart R, Pattnaik B, Thomson JA, Gamm DM (2011) Optic vesicle-like structures derived from human pluripotent stem cells facilitate a customized approach to retinal disease treatment. *Stem Cells* 29:1206–1218. <https://doi.org/10.1002/stem.674>
160. Garita-Hernandez M, Guibbal L, Toualbi L, Routet F, Chaffiol A, Winckler C, Harinquet M, Robert C, Fouquet S, Bellow S, Sahel JA, Goureau O, Duebel J, Dalkara D (2018) Optogenetic light sensors in human retinal organoids. *Front Neurosci* 12:789. <https://doi.org/10.3389/fnins.2018.00789>
161. Reinhard K, Tikidji-Hamburyan A, Seitter H, Idrees S, Mutter M, Benkner B, Münch TA (2014) Step-by-step instructions for retina recordings with perforated multi electrode arrays. *PLoS ONE* 9:e106148–e106148. <https://doi.org/10.1371/journal.pone.0106148>
162. Stett A, Egert U, Guenther E, Hofmann F, Meyer T, Nisch W, Haemmerle H (2003) Biological application of microelectrode arrays in drug discovery and basic research. *Anal Bioanal Chem* 377:486–495. <https://doi.org/10.1007/s00216-003-2149-x>
163. Singh R, Winkler P, Binette F, Petersen-Jones S, Nasonkin I (2021) Comparison of developmental dynamics in human fetal retina and human pluripotent stem cell-derived retinal tissue. *Stem Cells Dev* 30:399–417. <https://doi.org/10.1089/scd.2020.0085>
164. Young RW (1976) Visual cells and the concept of renewal. *Invest Ophthalmol Vis Sci* 15:700–725
165. Young RW, Bok D (1969) Participation of the retinal pigment epithelium in the rod outer segment renewal process. *J Cell Biol* 42:392–403. <https://doi.org/10.1083/jcb.42.2.392>
166. Kocaoglu OP, Liu Z, Zhang F, Kurokawa K, Jonnal RS, Miller DT (2016) Photoreceptor disc shedding in the living human eye. *Biomed Opt Express* 7:4554–4568. <https://doi.org/10.1364/BOE.7.004554>
167. Strauss O (2005) The retinal pigment epithelium in visual function. *Physiol Rev* 85:845–881. <https://doi.org/10.1152/physrev.00021.2004>
168. Kiser PD, Golczak M, Palczewski K (2014) Chemistry of the retinoid (visual) cycle. *Chem Rev* 114:194–232. <https://doi.org/10.1021/cr400107q>
169. Morshedian A, Kaylor JJ, Ng SY, Tsan A, Frederiksen R, Xu T, Yuan L, Sampath AP, Radu RA, Fain GL, Travis GH (2019) Light-driven regeneration of cone visual pigments through a mechanism involving RGR opsin in Muller glial cells. *Neuron* 102:1172–1183.e5. <https://doi.org/10.1016/j.neuron.2019.04.004>
170. Kay P, Yang YC, Paraoan L (2013) Directional protein secretion by the retinal pigment epithelium: roles in retinal health and the development of age-related macular degeneration. *J Cell Mol Med* 17:833–843. <https://doi.org/10.1111/jcmm.12070>
171. Raymond SM, Jackson IJ (1995) The retinal pigmented epithelium is required for development and maintenance of the mouse neural retina. *Curr Biol* 5:1286–1295. [https://doi.org/10.1016/s0960-9822\(95\)00255-7](https://doi.org/10.1016/s0960-9822(95)00255-7)
172. Sheedlo HJ, Nelson TH, Lin N, Rogers TA, Roque RS, Turner JE (1998) RPE secreted proteins and antibody influence photoreceptor cell survival and maturation. *Brain Res Dev Brain Res* 107:57–69. [https://doi.org/10.1016/s0165-3806\(97\)00219-8](https://doi.org/10.1016/s0165-3806(97)00219-8)
173. Achberger K, Probst C, Haderspeck J, Bolz S, Rogal J, Chuchuy J, Nikolova M, Cora V, Antkowiak L, Haq W, Shen N, Schenke-Layland K, Ueffing M, Liebau S, Loskill P (2019) Merging organoid and organ-on-a-chip technology to generate complex multi-layer tissue models in a human retina-on-a-chip platform. *Elife* 8:e46188. <https://doi.org/10.7554/eLife.46188>
174. Bringmann A, Syrbe S, Görner K, Kacza J, Francke M, Wiedemann P, Reichenbach A (2018) The primate fovea: structure, function and development. *Prog Retin Eye Res* 66:49–84. <https://doi.org/10.1016/j.preteyeres.2018.03.006>
175. da Silva S, Cepko CL (2017) Fgf8 expression and degradation of retinoic acid are required for patterning a high-acuity area in the retina. *Dev Cell* 42:68–81.e6. <https://doi.org/10.1016/j.devcel.2017.05.024>
176. Li G, Xie B, He L, Zhou T, Gao G, Liu S, Pan G, Ge J, Peng F, Zhong X (2018) Generation of retinal organoids with mature rods and cones from urine-derived human induced pluripotent stem cells. *Stem Cells Int* 2018:4968658. <https://doi.org/10.1155/2018/4968658>
177. Birey F, Andersen J, Makinson CD, Islam S, Wei W, Huber N, Fan HC, Metzler KRC, Panagiotakos G, Thom N, O'Rourke NA, Steinmetz LM, Bernstein JA, Hallmayer J, Huguenard JR, Pasca SP (2017) Assembly of functionally integrated human forebrain spheroids. *Nature* 545:54–59. <https://doi.org/10.1038/nature22330>
178. Ank YB, Buijsman W, Loessberg-Zahl J, Cuartas-Vélez C, Veenstra C, Logtenberg S, Grobink AM, Bergveld P, Gagliardi G, den Hollander AI, Bosschaart N, van den Berg A, Passier R, van der Meer AD (2021) Microfluidic organ-on-a-chip model of the outer blood-retinal barrier with clinically relevant read-outs for tissue permeability and vascular structure. *Lab Chip* 21:272–283. <https://doi.org/10.1039/d0lc00639d>
179. Wang L, Hiler D, Xu B, AlDiri I, Chen X, Zhou X, Griffiths L, Valentine M, Shirinifard A, Sablauer A, Thiagarajan S, Barabas ME, Zhang J, Johnson D, Frase S, Dyer MA (2018) Retinal cell type DNA methylation and histone modifications predict reprogramming efficiency and retinogenesis in 3D organoid cultures. *Cell Rep* 22:2601–2614. <https://doi.org/10.1016/j.celrep.2018.01.075>
180. DiStefano T, Chen HY, Panebianco C, Kaya KD, Brooks MJ, Gieser L, Morgan NY, Pohida T, Swaroop A (2018) Accelerated and improved differentiation of retinal organoids from pluripotent stem cells in rotating-wall vessel bioreactors. *Stem Cell Rep* 10:300–313. <https://doi.org/10.1016/j.stemcr.2017.11.001>
181. Kruzek K, Swaroop A (2020) Pluripotent stem cell-derived retinal organoids for disease modeling and development of therapies. *Stem Cells* 38:1206–1215. <https://doi.org/10.1002/stem.3239>
182. Regent F, Chen HY, Kelley RA, Qu Z, Swaroop A, Li T (2020) A simple and efficient method for generating human retinal organoids. *Mol Vis* 26:97–105
183. D'Costa K, Kosic M, Lam A, Moradipour A, Zhao Y, Radisic M (2020) Biomaterials and culture systems for development of organoid and organ-on-a-chip models. *Ann Biomed Eng* 48:2002–2027. <https://doi.org/10.1007/s10439-020-02498-w>
184. Georgiou M, Chichagova V, Hilgen G, Dorgau B, Sernagor E, Armstrong L, Lako M (2020) Room temperature shipment does not affect the biological activity of pluripotent stem cell-derived retinal organoids. *PLoS ONE* 15:e0233860. <https://doi.org/10.1371/journal.pone.0233860>
185. Reidel B, Thompson JW, Farsiu S, Moseley MA, Skiba NP, Arshavsky VY (2011) Proteomic profiling of a layered tissue reveals unique glycolytic specializations of photoreceptor cells. *Mol Cell Proteomics* 10(M110):002469. <https://doi.org/10.1074/mcp.M110.002469>

Publisher's Note Springer Nature remains neutral with regard to jurisdictional claims in published maps and institutional affiliations.